SHIMADZU
Excellence in Science

NEWS 01 2019

Weight reduction

New testing methodology
for composite material

Clear view in wet conditions

Polarizing sunglasses block the
glare from wet surfaces

Less expensive and easy

Analysis of dioxins in foods
and feeds using GC-MS/MS

MARKETS

- Chemical, Petrochemical, Biofuel and Energy
- Clinical
- Environment
- Food, Beverages, Agriculture
- Pharmaceutical
- Plastics and Rubber
- Automotive

Clear view in wet conditions

UV-Vis spectroscopy: Polarizing sunglasses block the glare from wet surfaces

As the days become longer, sunglasses are a common sight again. Today, there are no limits to design and color of frame and glasses.

But not all design choices are purely aesthetic: Yellow glasses for example enhance contrast while the advantage of green glasses is lower color distortion.

Figure 1: Investigated sunglasses. Upper half: Models without polarizing filters, lower half: Models with polarizing filters.

Important for the necessary protective functions are the shading (attenuation of the transmitted light) and the wavelength range covered. Both are optimized by the choice of base material and coating. Quality glasses block all light of wavelength 400 nm and below for complete UV protection.

A special case are polarizing sunglasses, promoted for watersports and car driving purposes, just to name two examples. In this case, polarizing filters are built into the glasses which block horizontally polarized light. Sunlight is generally unpolarized, but the reflection on a smooth surface causes a polarization horizontal to that surface. Polarizing filters are supposed to protect the user from this glare.

Polarization on a surface

Light can be described as an electromagnetic wave, as shown in figure 2, with propagation direction C, wavelength λ, electric field vector E and magnetic field vector B perpendicular to E. The direction of the electric field vector is also described as polarization. A beam of light is composed of many such waves with the same direction of propagation. Depending on the light source, the properties of these photons can be very different (e.g. sunlight) or uniform (e.g. laser).

The beam of light is polarized when some polarization directions are filtered out and one polarization direction becomes dominant. One example is reflection on a smooth surface, as shown in figure 3. The light with polarization horizontal to that surface is reflected to a higher degree [1], e.g. by snow or water, but also by the optical element of a UV-Vis spectrophotometer, such as a mirror or grating. The degree of polarization depends on the angle of incidence in both cases.

This polarization of the sample beam must be compensated for when a sample with polarizing properties is examined. A polarizer (figure 4, left side) is transparent only to light with one polarization direction and is used to enforce a complete polarization of the sample beam. By this, polarization effects (e.g. by reflection from the sample) are eliminated.

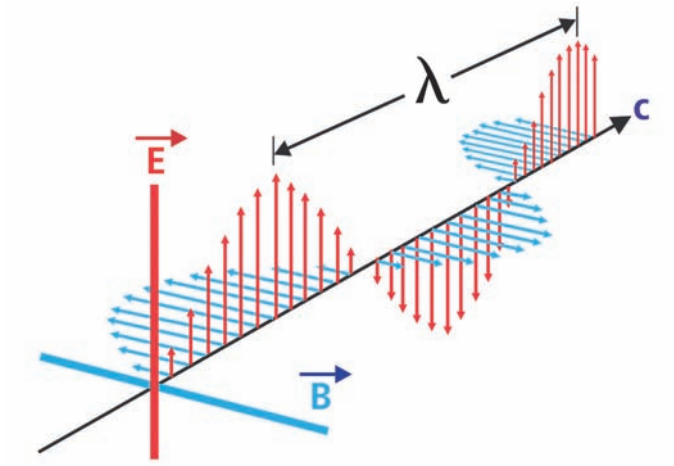

Figure 2: Vector representation of an electromagnetic wave with propagation direction C, wavelength λ, electric field vector E and magnetic field vector B.

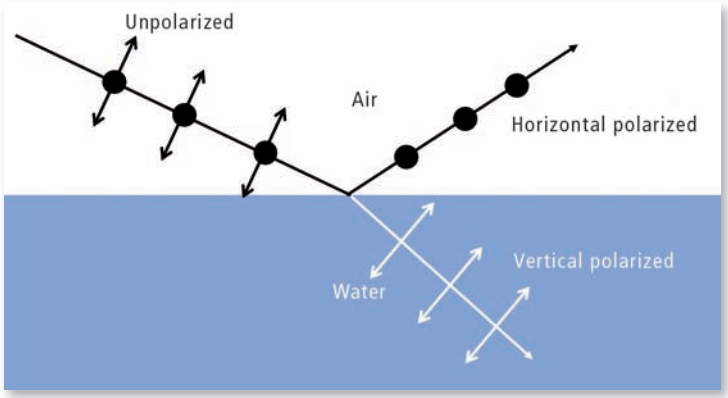

Figure 3: Polarization by reflection on a surface. Light with polarization vertical to the surface enters the surface, meaning that the horizontally polarized light is reflected. The degree of polarization depends on the angle of incidence.

A depolarizer (figure 4, right side) converts polarized light into completely unpolarized light [2].

Setup and samples

For the measurements described here, a Shimadzu UV-3600 Plus spectrophotometer was used. The baseplate of the rotating film holder accessory was used for mounting the polarizer and depolarizer. This setup is shown in figure 5 (page 4). To compare the effects of polarized and unpolarized light, a foil polarizer (spectral range 400 - 700 nm) and a Hanle depolarizer (spectral range 180 - 2,500 nm) were used.

Two different sunglasses with polarizing filters and two different sunglasses without polarizing filters were investigated. The samples were carefully positioned so that the frame didn't block the sample beam. Of each sample, the transmission spectrum was measured in the wavelength range of 400 - 700 nm in four different configurations:

- without any additional optics in the light path
- with unpolarized light (depolarizer in position A)

Figure 4: Polarizer (left) and depolarizer (right). The line on the polarizer mount indicates the polarization direction of the transmitted light.

- with vertical polarized light (polarizer set to 0° in position A)
- with horizontal polarized light (polarizer set to 90° in position A).

Polarizing filters for selective absorption

Figure 6 shows the transmission spectra of the sunglasses described above. The samples are labelled by their glass color as orange (upper left), green (upper right), black (lower left) and multicolored (lower right). The spectra are arranged analog to the photos of figure 1 (page 2).

Only the spectra of polarizing glasses without additional optics show peaks at 470, 580 and 665 nm. Transmission in these measurements is also below the values measured for the same glasses with a depolarizer in the light path. This shows that the sample beam is horizontally polarized to some degree. As the degree of polarization depends on the angle of incidence to the polarizing element, this absorption is only indirectly dependent on the wavelength. The spectra measured without depolarizer are influenced by such polarization effects.

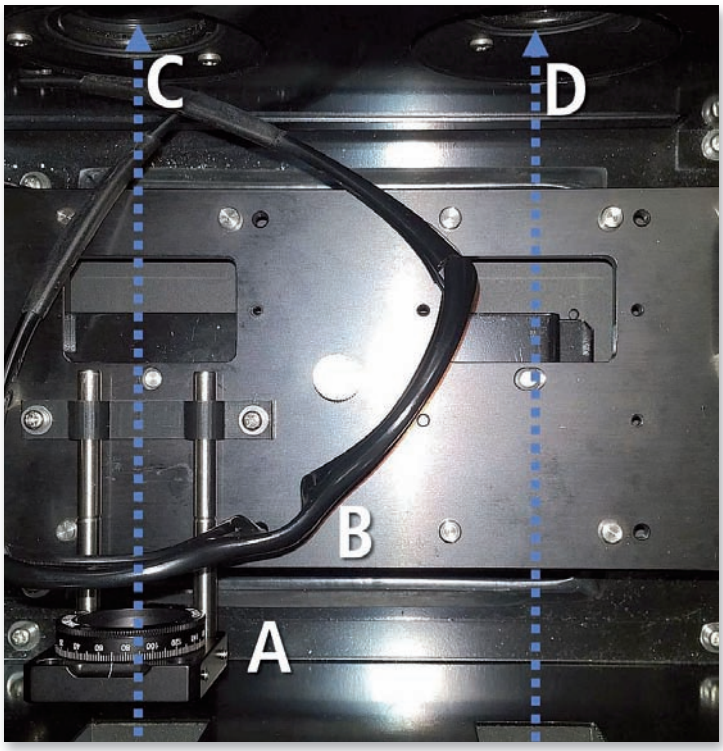

Figure 5: Experimental setup. A: Mounting position for polarizer or depolarizer, B: Sunglasses, C: Sample beam, D: Reference beam.

For the orange and green sunglasses, all four spectra are congruent. The polarization of the sample beam does not have any influence on the measurements. This is different to the spectra of the black and multicolored sunglasses. As expected from sunglasses promoted for watersports, the transmission for horizontally polarized light is very low. The black sunglasses show transmission values of around 20 % for vertical polarized light in this measurement range, but only 10 % for unpolarized light and less than 5 % for horizontal polarized light.

This effect is weaker with the multicolored sunglasses. The spectra measured with unpolarized and vertically polarized light are nearly congruent. The attenuation of horizontally polarized light is still remarkable though. The best attenuation is observed in the spectral range of 500 - 620 nm, while the black sunglasses show an even attenuation over the whole spectral range up to 650 nm.

Conclusion

Many projects in the optic industry are concerned with polarized light. Using a depolarizer will ensure that the sample is irradiated with completely unpolarized light. Measurement artifacts are therefore avoided and the true properties of polarizing samples are elucidated.

Literature

[1] https://en.wikipedia.org/wiki/Polarization_(waves)
[2] https://en.wikipedia.org/wiki/Depolarizer_(optics)

Further information on this article:
- Application: shimnet.shimadzu.local/product/Spectro/Spectro_UV/Application_Notes/SCA-100-022_Sunglasses.pdf

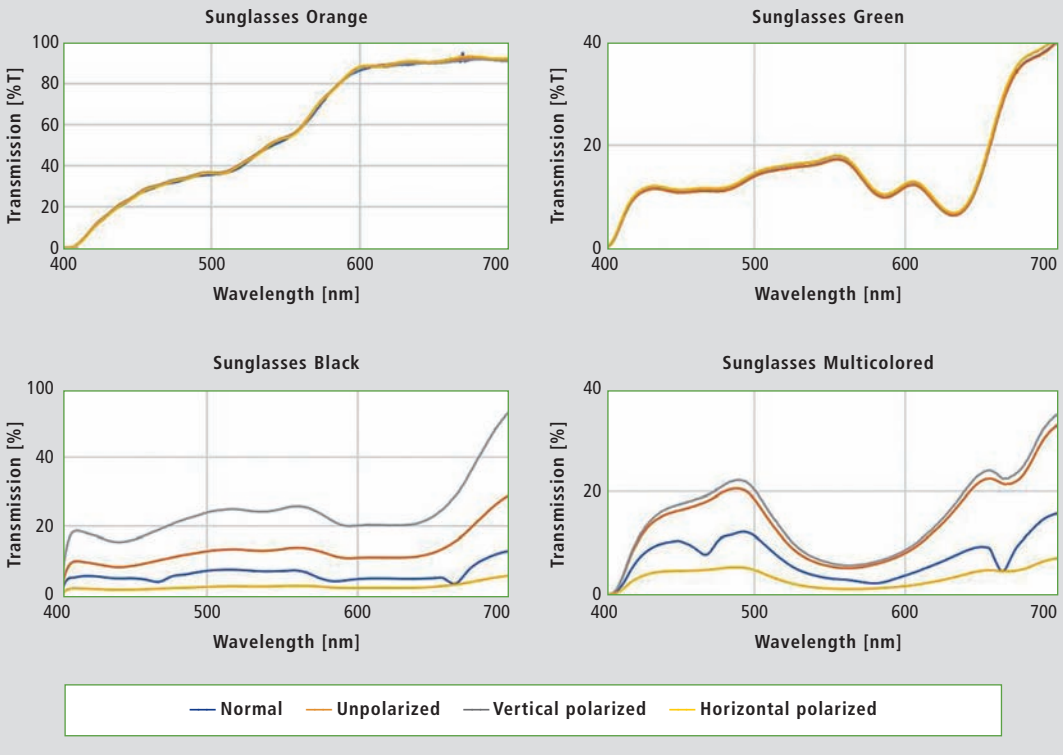

Figure 6: Transmission spectra of the four sunglasses from figure 1 (page 2), each measured in four configurations and in the spectral range of 400 - 700 nm. Upper half: Samples without polarizing filters, lower half: Samples with polarizing filters.

Mission for a good cause

Social Day 2018: Shimadzu Europe plants 1,500 new trees

The social day, at which Shimadzu employees support social projects, has become a tradition within the company since 2013. Once again, volunteers have been actively involved in their community and in December 2018 helped to reforest an area in the city forest of Duisburg with 1,500 new trees. This will contribute to the long-lasting woodlands development. So far, the heavily thinned out area was covered only with birch and bracken.

The 1,200 young European oak and 300 sweet chestnut, littleleaf linden and hornbeam have been selected to fit the natural tree species spectrum, growing well in the sandy soil. Forests with these indigenous trees serve as a habitat for many rare and endangered animals, plants and fungus species. Additionally, oak and linden trees are particularly long-lived, so future generations will also enjoy this biotope. The planted woodland is part of the Duisburg Sechs-Seen-Platte (Six Lakes Region), a recreational area with a network of hiking trails of 18 kilometers.

The two-three-year-old trees with a size of about 1.50 m were planted relatively densely, so they can decide among themselves which of them grows best in the first 20 to 30 years. This replicates nature that produces an unimaginably large number of seedling offspring by natural seeding from the mother trees, which evolve over the years so that only a few trees remain and their number continues to reduce further as they grow. Usually the trees prevail which secure the best spot in the sun over the longest period, receiving the most sunlight in the long term.

Social Responsibility

'Realizing wishes for the well-being of mankind and the Earth' is one of Shimadzu's established corporate principles. Engaging in community, society and the environment expresses this claim at the local level.

In the year of its 50th anniversary in Europe, Shimadzu gladly supported this long-term project and thanks all 30 participating employees of Shimadzu Germany and Shimadzu Europa for their individual social commitment.

What's in the water?

Water analysis of humic acid with fluorescence spectroscopy

Figure 1: Autumn view of a city park with a pond supplied with fresh water

Water is the basis of all life, all of nature and its habitats. When processed into food as drinking water, it's a substance that is strictly tested. However, water also has an important task in chemistry since it is a good solvent and absorbs many substances.

The most common way of water to enter the natural cycle is as rain into the ground and then into water bodies or deeper wells. It absorbs soil components and carries them in solution or as suspended particles. There are both visible and invisible portions.

Visible particles usually give the water an earthy color, an appearance that is normal for outdoor ponds or lakes (figure 1). However, if a slight tint in a bottle of drinking water is found, it is perceived purely subjectively as deviating from norm and experience. Drinking water is expected to be colorless and clear.

The warm summer of 2018 brought a supply of still mineral water with a slight tint (figure 2). This had to be investigated with fluorescence spectroscopy.

It is known from the literature that water can contain humic acid, a natural degradation product of organic sources such as leaves and grasses. This occurs naturally with open water, and the acid serves as food for living organisms in the water. Humic acid is not a stable molecule. It oxidizes through oxygen and decomposes chemically into tryptophan and L-tyrosine. It could be deduced from this reaction that if no more humic acid is present, the necessary amount of oxygen in the water is also consumed [1], [2], [3].

In the following application, it was interesting to determine the change in humic acid content by fluorescence spectroscopy. Humic acid, tryptophan and tyrosine show a fluorescence spectrum under excitation in the ultraviolet

Figure 2: Still mineral water with a slight coloration from a delivery in summer 2018

Fluorophores	Samples and references								
	Humic acid 20 mg/L	Tyrosine 1 mg/L	Tryptophan 1 mg/L	Bi-distilled	Mineral water	Well water, standing, garden hose	Well water, freshly pumped, garden hose	Pond water standing	Pond water with fresh water exchange
A	0	0	976	0	0	34	0	86.1	38.6
B	0	583	0	0	0	44.5	0	45.7	32
C1	100	0	0	0	27	34.9	36.6	24.9	82.6
C2	51	0	0	0	17	30	26.5	17.3	40

Table 1: Intensities of the fluorophores in the samples and references

range. Due to their chemical structure, the complex molecules have many ring systems, and individual electrons can be excited to energetically higher states. The energy absorbed in this way is released again via radiation of photons when the electron returns to its energetic ground state.

For this fluorescence analysis a rapid screening was used, ending in an EEM view (Excitation Emission Matrix). Fluorescence spectroscopy is a very sensitive and selective measurement technique. It can make traces of fluorescent-active substances visible in a mixture.

Samples

Various samples were collected for this study:

- A chemically pure water – double distilled,
- Well water, standing, from a garden hose,
- Well water, freshly pumped, from a garden hose,
- Pond water standing,
- Pond water with fresh water exchange, and
- Mineral water without carbon dioxide (still).

Reference materials were solutions of tyrosine (1 mg/L), tryptophan (1 mg/L) and humic acid (20 mg/L, pH 8 to 9).

All liquids used were transferred into a fluorescence cell. In the standard version, the cuvettes have four polished windows and a layer thickness of 10 x 10 mm. The quartz in this cuvette is fluorescence-free. The windows are needed because fluorescence is a scattered light which is detected at an angle of 90 degrees from the irradiation direction of the excitation source. The reference material was balanced and diluted with double distilled water. This water was also tested to exclude possible contamination (see figure 3).

Analysis of DOM in natural water

"Dissolved Organic Matter" was investigated with the Shimadzu RF-6000 fluorescence spectrophotometer.

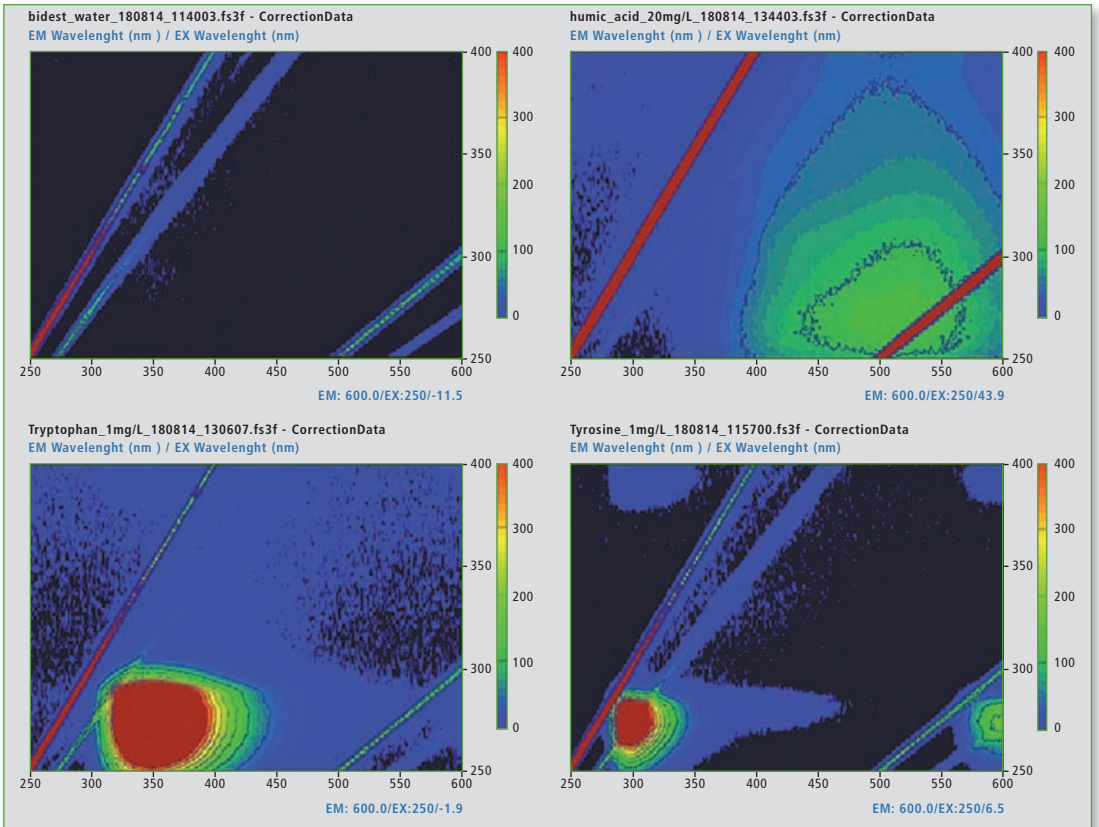

Figure 3: Representation of the EEM matrix of double distilled water (top left), humic acid (top right), tryptophan (bottom left) and L-tyrosine (bottom right), the scaling of the representation was set to 0 - 400 intensities (red corresponding to very intense, black up to no intensity).

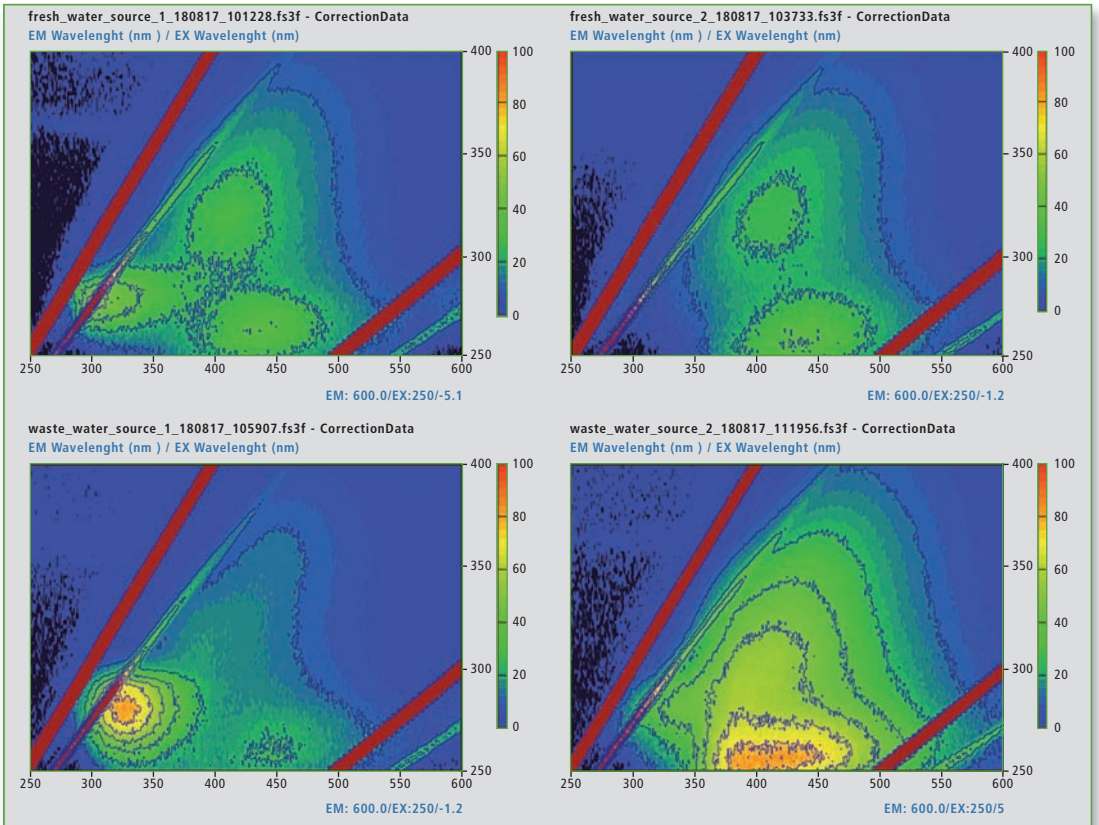

Figure 4: Representation of the EEM matrices of standing well water in a hose (top left), flowing well water from a hose (top right), standing pond water (bottom left) and flowing pond water (bottom right).

In a quick screening, EEM matrices of the samples and references were created. The EEM matrix is formed when the excitation wavelengths are increased slowly in small steps and the respective fluorescence spectrum is applied. Depending on the recording speed, it can take approx. 2 minutes (60,000 nm/s) or approx. 13 minutes (2,000 nm/s) to create the matrix.

From the reference measurements, it was possible to obtain the analytical wavelengths for the identification of the proteins involved. Distilled water shows no presence of a fluorophore, as was to be expected.

The excitation wavelength (EX) at 275 nm and the emission wavelength range (EM) at 340 - 381 nm were found for tryptophan. For L-tyrosine the EX are at 275 nm and EM at 310 - 320 nm. The humic acid has two active surfaces in the EEM at EX 300 - 370 nm and EM 400 - 500 nm, as well as EX 240 - 260 nm and an EM of 450 - 500 nm.

In the same way, the five samples from different sources were examined. All samples had lower concentrations than the reference material. It became apparent (figures 4 [page 7] and 5), that the mineral water contained a low concentration of a molecule similar to humic acid. In the standing waters, the signal group of humic acid has decreased strongly. Tryptophan and L-tyrosine-similar substances predominate. Both fresh waters, on the other hand, contain mostly proteins similar

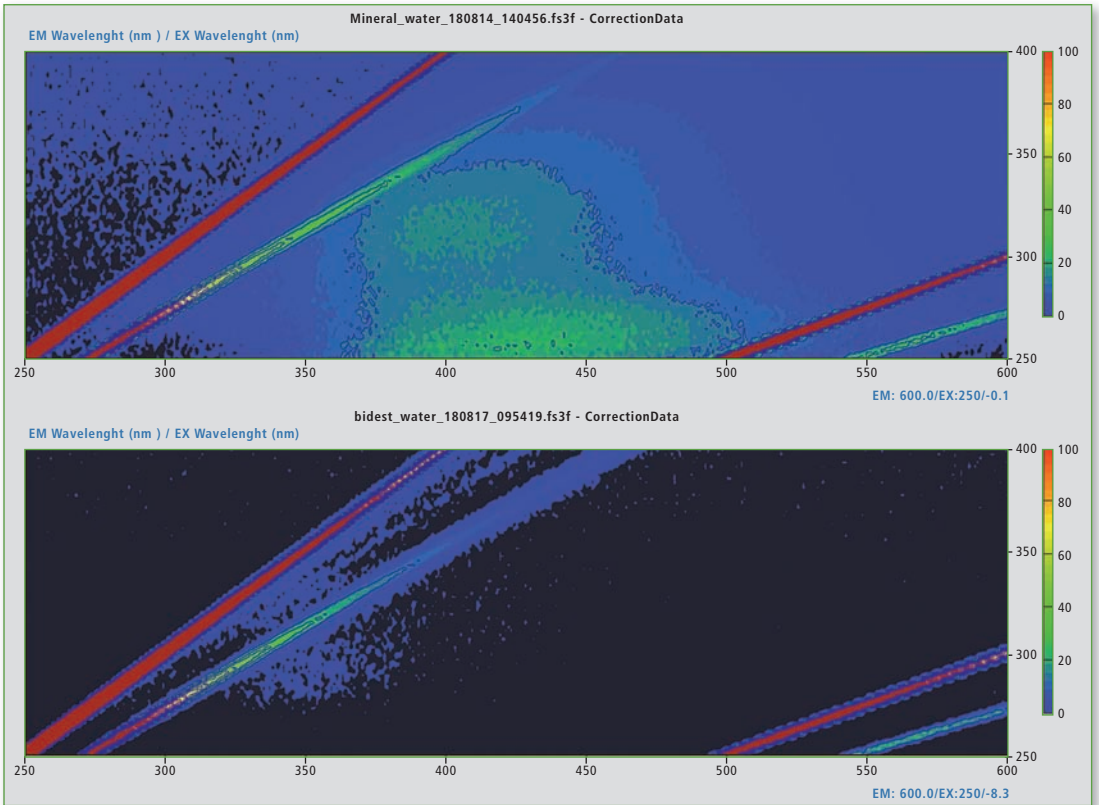

Figure 5: Comparison of the EEM matrices of still mineral water from the bottle (summer 2018) and double-distilled water from the laboratory. The mineral water exhibits fluorescence activity in the area of humic acid-like proteins.

to humic acid. Table 1 (page 6) shows the detected intensities of all samples and references involved to make the quantitative aspect visible.

Conclusion

The Excitation Emission Matrix (EEM) of fluorescence spectroscopy is a very fast technique for obtaining an overview of dissolved organic components (DOM) in water. With this option, the water quality can be monitored, for example, in wastewater treatment processes and also for contamination of natural water.

Literature

[1] Hudson, N., Baker, A. and Reynolds, D. (2007). Fluorescence analysis of dissolved organic matter in natural, waste and polluted waters – a review. River Research and Applications 23: 631-649.

[2] Yan, Y., Li, H. and Myrick, M. L. (2000). Fluorescence fingerprint of waters: excitation-emission matrix spectroscopy as a tracking tool. Applied Spectroscopy 54(10): 1539-1542.

[3] AD-0133, Shimadzu Asia Pacific, 2016

Further information on this article:

- Application: AD-0133: Excitation-Emission Matrix (EEM) Fluorescence Spectroscopy for Analysis of Dissolved Organic Matter (DOM) in Natural Water and Wastewaters
- Application: SCA_105_010: Dissolved organic matter analysis (DOM) and its appearance under different environmental conditions – fluorescence EEM matrices of different sources

Hard x-ray for soft water

Quality control of zeolites for washing powder with EDX-8000P

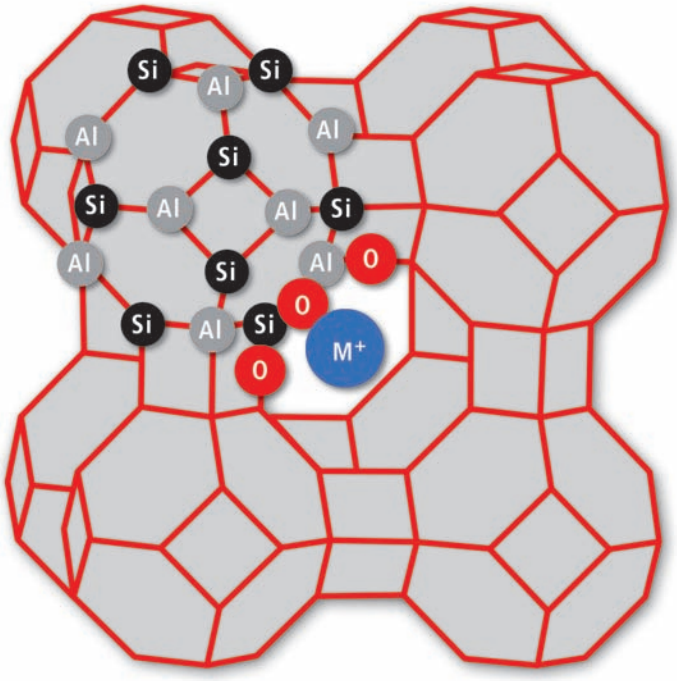

Figure 1: Structure of Zeolite A. Al and Si atoms (nodes) are connected by shared O atoms (lines), leading to a cage of alternating AlO_4 and SiO_4 tetrahedrons. Only some atoms are labelled to indicate the binding motif.

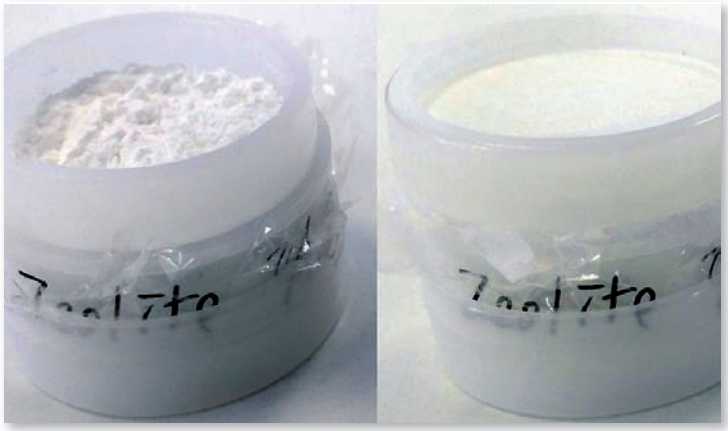

Figure 2: Zeolite powder prepared for EDX measurement. Left: open cup, right: sealed cup for vacuum measurements.

Many washing powders contain zeolites for water softening. This role was fulfilled in the past by phosphates, leading to a notorious growth of algae and severe damage of aquatic ecosystems. Even though natural zeolites exist, they are specifically synthesized with defined stoichiometry and structure [1]. One widely used example is Zeolite A with an equal content of alumina and silicone. The advantage for technical applications is a well-defined anionic cage structure made from $([AlO_2]_{12}[SiO_2]_{12})^{12-}$ blocks as shown in figure 1.

Molecules such as water that are small enough to enter the pores are bound there until the zeolite is heated. The effective pore diameter for use as molecular sieve is on the scale of 0.3 - 0.5 nm and depends on the cations bound to the anionic cage, since they block the pores to some degree depending on their size, charge and binding force.

For the application as water softener, only sodium and potassium are valid cations. During the laundry, they are exchanged easily by calcium or magnesium from the hard water, which have a higher binding force to the zeolite cage. Without free Ca^{2+} or Mg^{2+}, the formation of lime is prevented. To ensure the best product quality for each target application, the elemental composition (aluminum (Al), silicon (Si), sodium (Na) and possibly other elements) of these zeolites must be controlled.

Easy sample preparation

A common method for precise elemental analysis is inductively coupled plasma optical emission spectroscopy (ICP-OES or short ICPE). For mineral samples, such as zeolites, a thorough digestion is needed. Sample preparation takes some time and requires the use of chemicals such as hydrofluoric acid.

A fast alternative for routine quality checks is energy-dispersive x-ray fluorescence spectroscopy (EDX), e.g. with the EDX-8000P, a system penetrating samples with so-called hard x-rays of up to 50 keV. Here, the zeolite powder is filled in a special sample cup without pretreatment. Digestion of the sample is not required, and measurement time is on the scale of a few minutes including preparation.

The EDX-8000P detector is optimized for light elements such as sodium, aluminum and silicon. For this measurement under vacuum condition, the cups are closed by a seal permeable to air to prevent bursting of the cup by the sudden pressure change and spilling of the sample.

Quick measurements

The EDX-8000P has another advantage for this application: the sample composition can be determined by fundamental parameters (FP) methods without the need for standards.

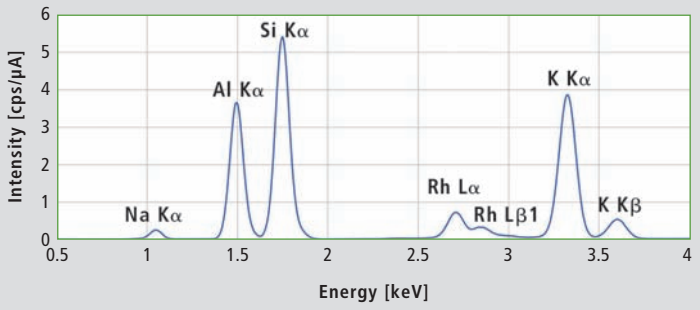

Figure 3: EDX spectrum of Zeolite A3 sample 1 at 15 kV tube voltage (C - Sc channel), 100 s live time and vacuum. The rhodium lines are scattered radiation from the x-ray tube.

Two such fundamental parameters are the order number and concentration of the elements included, which are given as results from the intensities of characteristic lines. Other fundamental parameters, like the sample shape, density or fixed concentrations, are either added manually or calculated from scatter peaks to support the algorithm.

FP methods are used for quick screening and depend strongly on how well the sample is described within the FP model. A higher quality quantitation of the elements is possible using calibration curves. Here, four samples of Zeolite 3A with different ratios of sodium to potassium were analyzed with an FP method and a quantitative method calibrated with ICPE results.

Figure 3 shows a typical EDX-spectrum of a synthetic zeolite after 100 seconds measurement time. All peaks detected over the defined measurement range are fitted and analyzed by an FP method. The rhodium lines are background from the x-ray tube and not used for the quantitative analysis.

Table 1 compares ICPE results given by the manufacturer of the samples to semi-quantitative and quantitative EDX measurements for all Zeolite 3A samples.

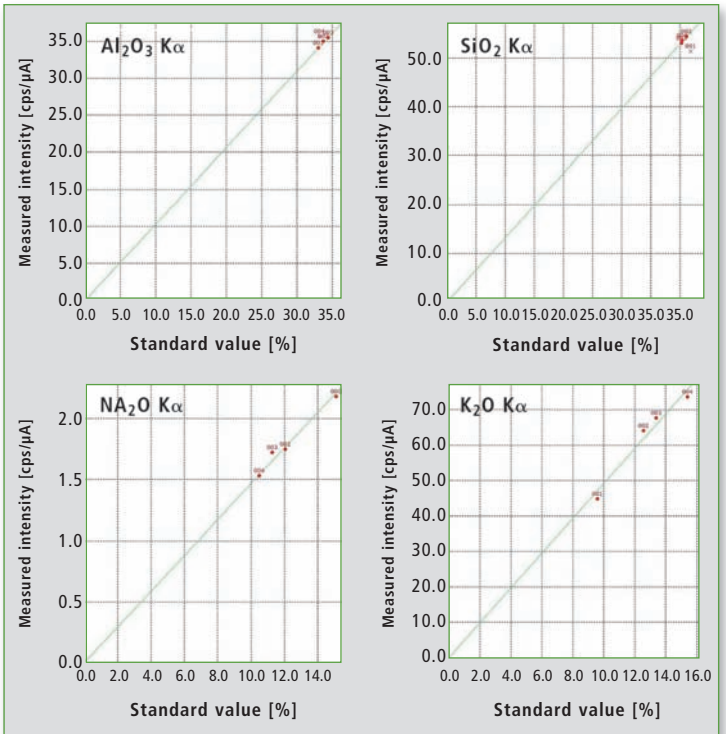

Figure 4: Calibration curves for the EDX method from table 1

The FP values for aluminum and silicon show a good match with the ICPE values, while the values for sodium and especially potassium show a bigger deviation. With the calibration curve method, only a small deviation from the ICPE values was found for all oxides.

To calibrate the EDX method, ICPE results of the same samples were used as standards. Calibration curves are shown in figure 4. While quantitation of aluminum and silicon by this calibration curve method seems to be inferior to the FP method at first glance, all standards had nearly identical contents of these elements, so there was not enough difference in intensity for a linear fit.

Matrix corrections

One important raw material for zeolite is the aluminum or bauxite, where the content of aluminum and undesired oxides must be monitored to optimize the process parameters. The analytical methods used for artificial zeolites are easily adopted for the quality check of natural bauxite. The possible influence of other oxides on the aluminum intensity must however be considered.

To show the effect of different matrix corrections, table 2 lists the results for five different samples of bauxite measured with different methods. The same samples were used as standards. Iron was found to be the interfering element in the case of aluminum in bauxite. This was derived from the observation that the change of the aluminum line intensities in samples with constant concentration of aluminum correlated to a change of the iron concentration.

To test the matrix correction, the De Jongh (dj) method [2] was used with one element for calculation of the correction factor. Each element was applied once for the correction and the aluminum concentration in each sample was recalculated once with each method. Table 3 shows the coefficient and average deviation from the ICPE value for each correcting element. As expected, the best results are found with iron as element for the correction.

For the mean deviation shown in table 3, relative deviation of each EDX value from the ICPE value of the same sample was calculated for each method and sample (see formula 1 page 11).

The average of these deviations over all samples was then calculated for each method (see formula 2 page 11).

When the interfering element is hard to identify, testing different corrections as in this example and finding the method with the smallest deviation is a good starting point. The correcting element should have a small coefficient (±0.001) to avoid overcompensation.

Conclusion

The EDX-8000P is the ideal instrument for quick quality checks. The fundamental parameters method can be enhanced by additional data, e.g. from loss of ignition measurements to measure unknown samples without the need for calibration. Using matrix corrections, analysis of more complicated minerals is possible. This way, the EDX method applying hard x-rays supports applications for water softening.

Acknowledgements

We gratefully acknowledge the assistance and supply of samples from our colleagues in Shimadzu d.o.o. Sarajevo, Bosnia and Herzegovina.

Literature

[1] Zeolithe – Eigenschaften und technische Anwendungen, Lothar Puppe, Chemie in unserer Zeit 1986, https://doi.org/10.1002/ciuz.19860200404

[2] X-ray fluorescence analysis applying theoretical matrix corrections. Stainless steel, Willy K. De Jongh, X-Ray Spectrometry 1973, https://doi.org/10.1002/xrs.1300020404

Concentration in %wgt												
Sample	Zeolite 3A sample 1			Zeolite 3A sample 2			Zeolite 3A sample 3			Zeolite 3A sample 4		
Method	ICPE	FP	Cal.	ICPE	FP	Cal.	ICPE	FP	Cal.	ICPE	FP	Cal.
Al_2O_3	33.06	33.34	34.05	33.77	32.32	34.00	34.67	32.49	34.38	33.18	32.33	34.68
SiO_2	41.90	40.78	40.24	41.90	40.70	41.20	40.34	39.57	40.33	40.44	39.55	40.71
Na_2O	15.09	13.86	15.38	12.05	10.85	11.89	11.27	10.81	11.69	10.50	9.67	10.36
K_2O	9.59	11.98	9.68	12.57	16.02	13.04	13.39	17.03	13.72	15.42	18.29	14.86

Table 1: Comparison of the results for Al_2O_3, SiO_2, Na_2O and K_2O for different zeolite samples and methods. All elements are defined as oxides for a better description of the mineral sample.

Concentration of Al_2O_3 in %wgt.					
	Baux 1	Baux 2	Baux 3	Baux 4	Baux 5
ICPE	78.25	59.58	60.77	62.63	66.78
FP	84.02	68.75	67.34	68.69	67.63
Cal. (no corr.)	74.22	59.90	65.03	67.08	63.71
Cal. (Si corr.)	75.49	57.60	64.66	67.09	63.64
Cal. (no corr.)	77.45	58.85	65.33	39.84	59.80
Cal. (Ti corr.)	77.43	56.43	60.44	61.29	61.16
Cal. (Fe corr.)	77.14	61.29	61.40	65.13	61.49

Table 2: Aluminum content in five different samples of bauxite, measured with different methods. The calibrated EDX methods differ only in the element used for calculation in the dj matrix correction.

Matrix correction for Al_2O_3		
Element	Coeff.	Mean deviation
none	none	4.80 %
Si	-0.003	4.94 %
Ca	-0.054	15.63 %
Ti	0.137	3.71 %
Fe	-0.007	3.54 %

Table 3: Elements und coefficients for the dj matrix correction from table 2 with corresponding mean deviation from ICPE values

$$Dev\ (Baux1, FE) = \frac{EDX(Baux1, FE) - ICPE(Baux1)}{ICPE(Baux1)} \cdot 100\ \%$$

Formula 1: Sample deviation

$$Dev\ (FE) = \frac{Dev(Baux1, FE) + Dev(Baux2, FE) + \ldots}{5}$$

Formula 2: Average deviation – calculated for each method

Purification made easy

Preparative purification of Ibuprofen and its related substances by Prominence UFPLC

Pharmaceutical companies are developing compounds of increased complexity – drugs with numerous functional groups in a single molecule, polymeric compounds, biopharmaceuticals such as peptides, proteins and many others – that must be purified, in production quantities. Regulatory agencies continue to press for more stringent requirements in purity of pharmaceutical products and, especially, drug substances. An acute need exists for other tools in addition to crystallization, the classic technique for purification, to address a growing number of purification problems.

Currently, preparative HPLC is the most powerful and versatile method for purification tasks in the pharmaceutical industry. The Prominence Ultra Fast Preparative and Purification Liquid Chromatograph (UFPLC) enables substantial labor savings in preparative purification.

This happens by automation not only of fractionation of the target compound but also the related processes of concentration, purification and recovery. This article introduces an example of preparative purification of a mixed sample of the pharmaceutical compound Ibuprofen and its analogs using Shimadzu's UFPLC Advanced System (figure 1) [1].

Procedures of preparative purification using the Shimadzu UFPLC system

UFPLC automatically performs the various processes related to preparative isolation of target compounds using a combination of preparative LC and trapping columns. Details of these processes are as follows:

1. separation of target compounds in complex sample by preparative LC and introduction into trapping columns
2. replacement of solvent in trapping columns with ultrapure water
3. elution of target compounds from trapping columns by organic solvent.

An outline of the respective processes is shown in figure 2.

The system integrates preparative LC with fraction trapping for up to five compounds of interest. It is controlled by a dedicated walk-up software designed to simplify the workflow also for non-expert users. It allows to easily set conditions for chromatographic separation and isolation of target compounds, trapping, eluting and collecting highly purified compounds in as little as 90 minutes. For applications involving the isolation of low concentration targets, replicate injection and collection to the same trapping column to increase the amount of compound trapped on column prior to elution is easily accomplished.

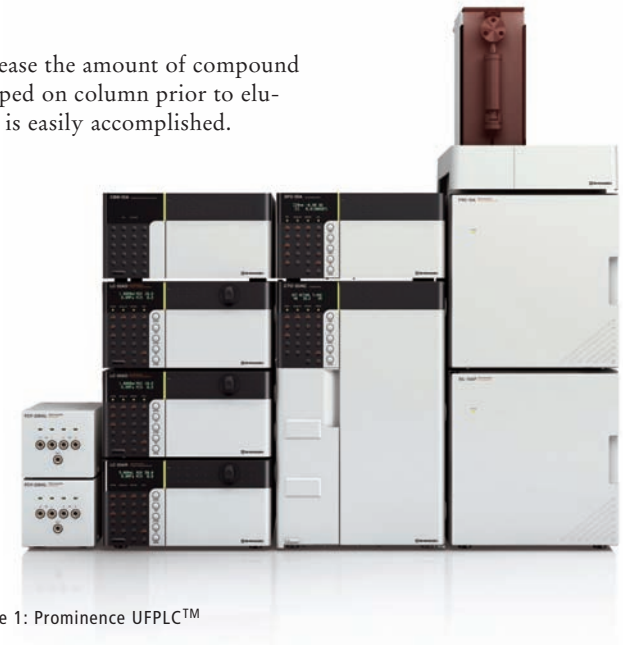

Figure 1: Prominence UFPLC™

High purity compounds, optionally recovered as a free base

The Prominence UFPLC eliminates some of the problems associated with conventional prep LC, especially poor purity of collected compounds due to mobile phase additives, which become contaminants in the final collected fraction and inhibit powderization. Shimadzu's "Shim-pack C2P-H" trapping column strongly retains target compounds, allowing unwanted organic solvents, water and additives to be flushed away. Additionally, rinsing the column with an aqueous ammonia solution after trapping allows compounds to be recovered as free bases which are generally easier to powderize, typically providing better quality results when used in drug screening and pharmacokinetic studies. All eluted compounds are finally collected in a highly volatile organic solvent, which reduces fraction dry-down time by up to 90 % compared to conventional LC fractions.

Preparative purification of Ibuprofen and its analogs

Ibuprofen is one type of nonsteroidal anti-inflammatory drug (NSAID) used as a fever-reducing drug and analgesic. The United States Pharmacopeia (USP) provides analytical methods for Ibuprofen and its analog 4-isobutylacetophenone, using valerophenone as an internal standard [2]. This article describes preparative purification of these three components using the Shimadzu UFPLC system (figure 3). Preparative LC and purification conditions are displayed in table 1.

Figure 4 shows the preparative LC chromatogram of the mixed solution of Ibuprofen and related compounds. It was prepared by dissolving the three target com-

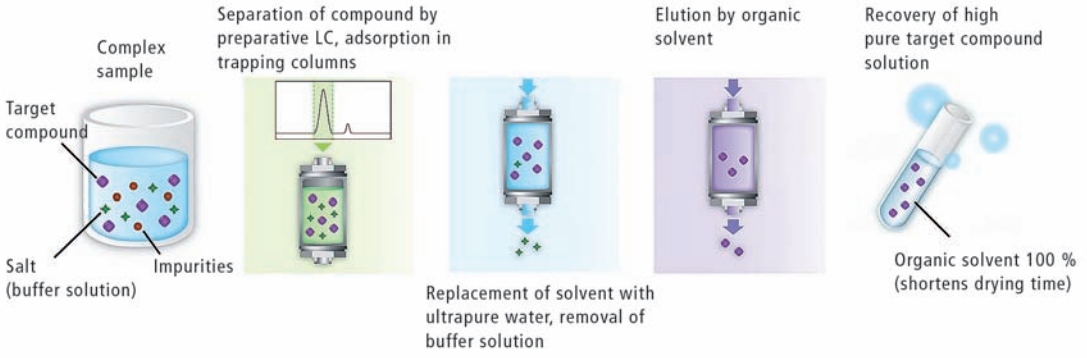

Figure 2: Prominence UFPLC™ workflow of fractionation, concentration, purification and elution

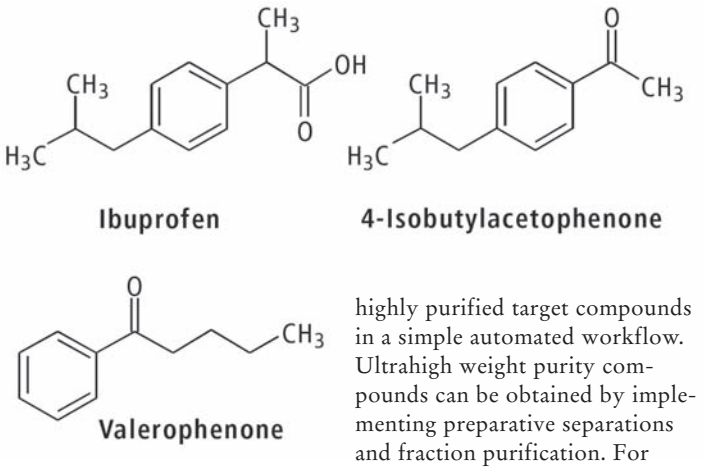

Figure 3: Chemical structures of Ibuprofen and related compounds

pounds with mobile phases to a concentration of 5,000 mg/L.

Verification of purity of Ibuprofen and its analogs

The fractions of Ibuprofen, valerophenone and 4-isobutylacetophenone collected by UFPLC were analyzed by standard HPLC to verify the purity of the compounds. Table 2 shows the analytical conditions and figure 5 shows the chromatograms obtained for each fraction. Purities of the target compounds contained in each fraction determined by area normalization at UV 230 are listed in table 3.

Conclusion

Prominence UFPLC Ultra-Fast Preparative and Purification Liquid Chromatograph was shown to enable fast recovery of highly purified target compounds in a simple automated workflow. Ultrahigh weight purity compounds can be obtained by implementing preparative separations and fraction purification. For powderization of the pure sample, an extremely long drying time is necessary using conventional reversed-phase preparative LC, due to a high amount of water in the mobile phase. Moreover, in cases where a nonvolatile buffer solution is used, the salt can precipitate after drying. In preparative purification using UFPLC, it is possible to remove the nonvolatile salt used in the separation process, as desalting is performed in the trapping columns. Drying time is substantially reduced by use of organic solvent for sample recovery from the trapping columns, contributing greatly to improved efficiency in any application requiring preparative purification.

Literature

[1] N. Kosuke, Shimadzu Application News No. L526, Preparative Purification of Ibuprofen and Its Related Substances by Prominence UFPLC
[2] USP Monograph for Ibuprofen

Preparative LC conditions	
Column	Shim-pack™ VP-ODS (250 × 10 mm, 5 µm)
Mobile phase	A: 1 % (wt/v) chloroacetic acid (pH 3.0) B: Acetonitrile A/B = 2/3 (v/v)
Flow rate	9.0 mL/min
Column Temperature	Ambient
Injection volume	100 µL
Detection	UV 230 nm
Rinse conditions	
Column	Shim-pack™ C2P-H (30 × 20 mm, 25 µm)
Rinse solvent	A: 2 % (v/v) acetonitrile aq. sol., B: water
Time program	A: 15 mL/min (0 - 2 min) → A: 8 mL/min (2.01 - 4 min) → B: 8 mL/min (4.01-8 min)
Elution conditions	
Eluent	Acetonitrile
Flow rate	4.5 mL/min
Detection	UV 230 nm

Table 1: Conditions of preparative LC separation and purification by UFPLC system

Analytical LC conditions	
Column	Shim-pack™ VP-ODS (250 × 4.6 mm, 5 µm)
Mobile phase	A: 1 % (wt/v) chloroacetic acid (pH 3.0) B: acetonitrile A/B = 2/3 (v/v)
Flow rate	2.0 mL/min
Column Temperature	30 °C
Injection volume	10 µL
Detection	UV 230 nm

Table 2: Conditions of analytical HPLC separation of purified fractions

Compounds	Area %
Ibuprofen	99.2
Valerophenone	99.6
4-Isobutylacetophenone	99.8

Table 3: Purities of target compounds contained in collected fractions (area percentage, UV 230 nm)

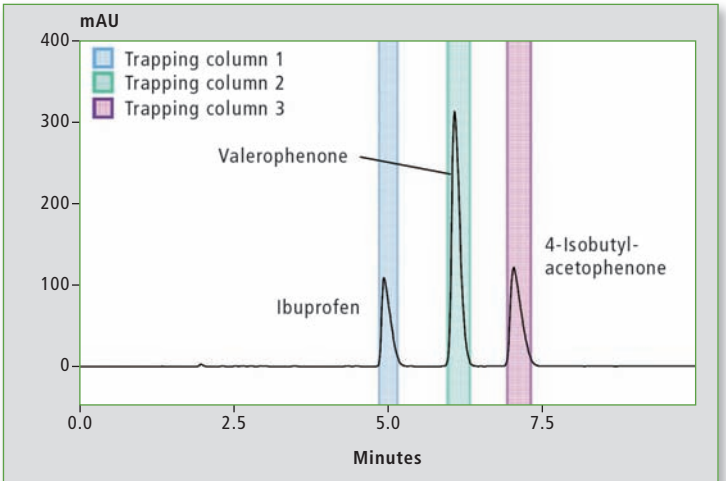

Figure 4: Preparative LC chromatogram of Ibuprofen and its analogs (UFPLC)

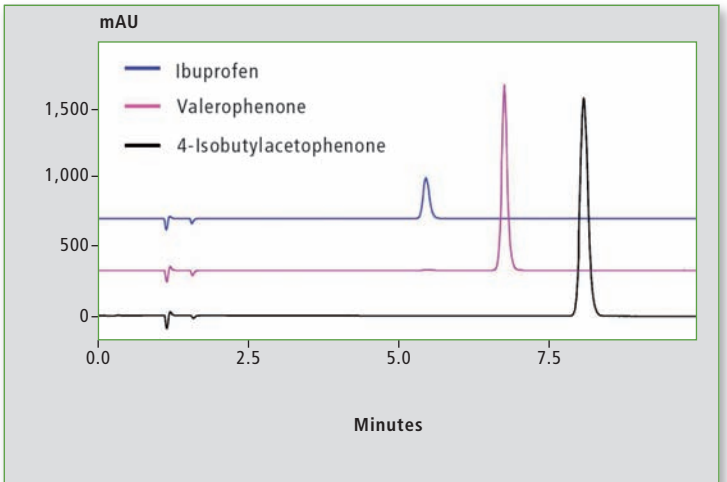

Figure 5: HPLC analysis of Ibuprofen and related compounds in fractions obtained by UFPLC

New anti-doping method for equestrian sports

Application of LCMS-8050 to quantify capsaicin and dihydrocapsaicin in horse serum

Members of research team

The Institute of Toxicological Research at Wroclaw Medical University in Poland routinely analyzes biological samples and evidence material on commission of the police, the prosecutor's office and the courts. Research encompasses both targeted and screening analyses including pharmaceuticals, drugs of abuse, new psychoactive substances, alcohols, volatile substances, anabolics and many others. The Institute is also interested in developing new methods of analysis for specific needs of customers from scientific fields, industries, veterinary medicine and medicine.

The Equine Internal Medicine Unit, part of the Department of Internal Disease with Clinic for Horses, Dogs and Cats, is a scientific group focused on clinical work, teaching and research in the field of internal diseases of horses. Main current research of group members includes asthma, metabolic and endocrine diseases and kidney failure of horses. Application possibilities of innovative biomarkers in diagnostics of internal diseases of horses are also investigated.

Strong analgesic properties of Capsicum peppers

Capsaicin and dihydrocapsaicin, alkaloids from Capsicum peppers, are used in medicine and veterinary medicine due to their strong analgesic properties. Local analgesic effect is related to defunctionalization of nerve endings. In the case of horses, both capsaicin and dihydrocapsaicin are used as analgesic and warming gels or ointment. They are widely used in treatment of lameness and limb localized pain. Due to strong analgesic properties and fast action, capsaicin has been placed on the Equine Prohibited Substances List created by the International Federation for Equestrian Sports.

Y. You et al. [1] in 2013 proved the possibility of using UHPLC-MS-MS for the detection of capsaicin in plasma samples. The method described is fast, selective, sensitive, reproducible, reliable and fully validated.

The aim of this papers' [2] research was to determine the time limit for the detection of capsaicin and dihydrocapsaicin after long-term use of gel containing capsaicin on horses. Of particular interest was to determine how soon after prolonged use of ointment or gel with capsaicin in pain treatment (following manufacturer application recommendations), horses would be able to

Members of research team

take part in competition bearing in mind the anti-doping regulations applied in equestrian sports.

Sample preparation

A serum sample (200 µL) was transferred into a 2 mL polypropylene tube. 20 µL of an internal standard solution (methanol solution of phenacetin, 100 ng/mL) was added. A liquid-liquid extraction using dichloromethane (1 mL) was carried out for five minutes. After shaking, samples were centrifuged at 10,000 rpm for five minutes. The organic phase was transferred into a clean 2 mL tube and evaporated to dryness under a stream of nitrogen at 40 °C. The extract was dissolved in 25 µL of methanol, transferred to an inert glass insert and analyzed using UHPLC-QqQ-MS/MS.

UHPLC-MS/MS analysis

Analysis was performed using a Nexera X2 UHPLC system coupled with an LCMS-8050 triple quadrupole mass spectrometer with ESI in positive ionization. The analytes were then quantified by multiple reaction monitoring (MRM). MRM transitions were m/z 180.30 → 110.05; 180.30 → 93.10; 180.30 → 65.05 for phenacetin, m/z 306.10 → 137.05; 306.10 → 94.10; 306.10 → 122.05 for capsaicin and m/z 308.40 → 137.10; 308.40 → 94.10; 308.40 → 122.10 for dihydrocapsaicin. The analytes were separated using a C_{18} 1.7 µm, 2.1 x 50 mm column at 40 °C. A combination of 10 mM ammonium formate / 0.1 % formic acid in water (A) and 0.1 % formic acid in acetonitrile (B) was used as mobile phase. Injection volume was 1 µL.

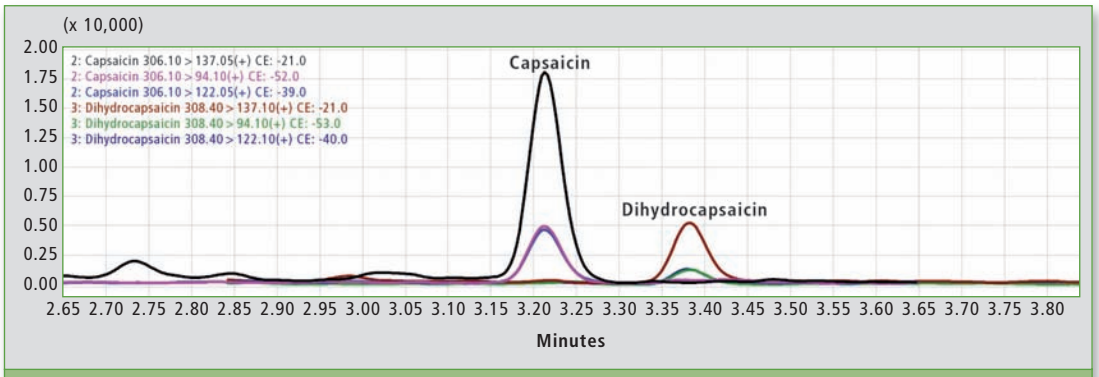

Figure 1: MRM of capsaicin and dihydrocapsaicin in blank equine serum at concentration of 1 pg/mL

Results

The limits of quantification of the analysis were 0.5 pg/mL for capsaicin and 1 pg/mL for dihydrocapsaicin. Figure 1 shows the chromatogram of pretreated horse serum containing capsaicin (1 pg/mL) and dihydrocapsaicin (1 pg/mL).

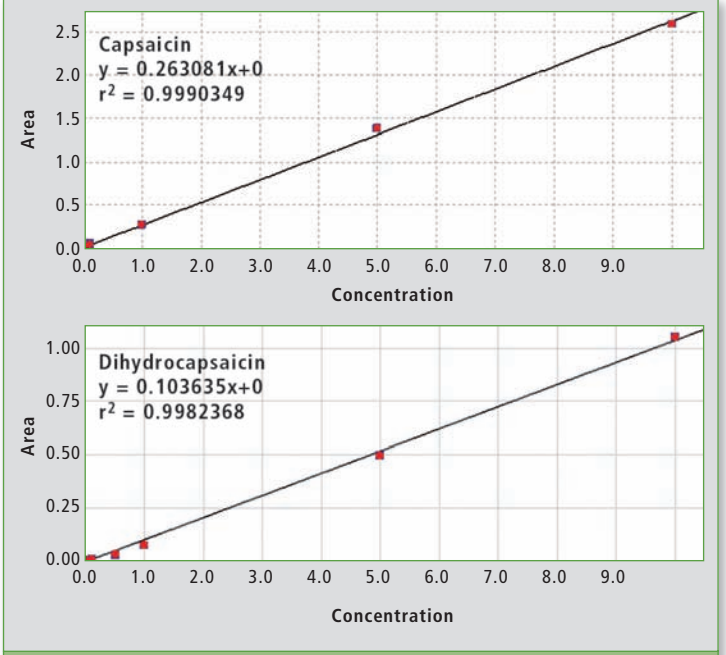

Figure 2: Calibration curves of capsaicin (above) and dihydrocapsaicin (below)

Y. You et al. research from 2013 on capsaicin and dihydrocapsaicin concentrations in equine plasma [1] has proven that after application of paste containing 0.025 % of capsaicin, both capsaicin and dihydrocapsaicin occurred in plasma, with a concentration of nearly 242 and 155 pg/mL respectively in two hours, but after 24 hours the concentrations declined to nearly 5 and 3 pg/mL, respectively. By reaching LOQ at 0,5 pg/mL and 1 pg/mL level, the method presented therefore enables effective detection of capsaicin even after 24 hours following application of gels containing this compound.

Very good linearity was achieved in the concentration range from 0.5 to 1,000 pg/mL (capsaicin) and 1 to 1,000 pg/mL (dihydrocapsaicin). Calibration curves and linear regression coefficients are shown in figure 2.

Real samples analysis

The method described was successfully applied for the detection of capsaicin and dihydrocapsaicin in horse serum following long-term local administration [2].

Conclusions

The undoubted advantages of the method presented are its simplicity, high sensitivity and the fast sample preparation procedure. The possibility of detection of capsaicin and its metabolite in concentrations from 0,5 pg/mL respectively 1 pg/mL enables the effective fight against this kind of doping in equestrian sports. Capsaicin also has more applications, so after small modifications, the method described can be used for determination of capsaicin and dihydrocapsaicin in chili peppers, self-defense weapons or biological samples collected from individuals exposed to these substances.

Authors

Paweł Szpot, Marcin Zawadzki, Marta Siczek, Agnieszka Zak, Natalia Siwinska, Malwina Słowikowska, Artur Niedzwiedz
The Equine Internal Medicine Unit, part of the Department of Internal Disease with Clinic for Horses, Dogs and Cats, Wrocław, Poland

Literature

1. Y. You, C. E. Uboh, L. R. Soma, F. Guan, D. Taylor, X. Li, Y. Liu, J. Chen: Validated UHPLC–MS-MS Method for Rapid Analysis of Capsaicin and Dihydrocapsaicin in Equine Plasma for Doping Control, Journal of Analytical Toxicology (2013) 37(2) 122-132. DOI 10.1093/jat/bks098.
2. A. Zak, N. Siwinska, M. Slowikowska, H. Borowicz, P. Szpot, M. Zawadzki and A. Niedzwiedz: The detection of capsaicin and dihydrocapsaicin in horse serum following long-term local administration BMC Veterinary Research (2018) 14:193. DOI 10.1186/s12917-018-1518-9

GCMS-TQ8050 NX

Less expensive with easier handling

Analysis of dioxins in foods and feeds using GC-MS/MS

Persistent organic pollutants (POPs) are semi-volatile and can be detected worldwide, even in remote regions. They bioaccumulate with potential negative influence on environment and human health. To a varying degree, these organic compounds resist photolytic, biological and chemical degradation.

POPs in foods and feeds can be analyzed with several methods. Dioxins are particularly toxic even for POPs, so quantitative analysis is required down to low concentrations. Until recently, the analysis of dioxins was performed using high-resolution GC-HRMS, which provides highly accurate quantitation. However, triple quadrupole GC-MS/MS is less expensive and easier to handle than GC-HRMS, so its use is increasingly being investigated.

In recent years, the quantitative accuracy of GC-MS/MS has improved significantly. Accordingly, the use of this analysis method has been officially recognized in the EU (EU589/2014, 644/2017). However, to change from GC-HRMS to GC-MS/MS it is necessary to compare their respective quantitative abilities.

The Shimadzu GCMS-TQ8050 NX triple quadrupole mass spec-

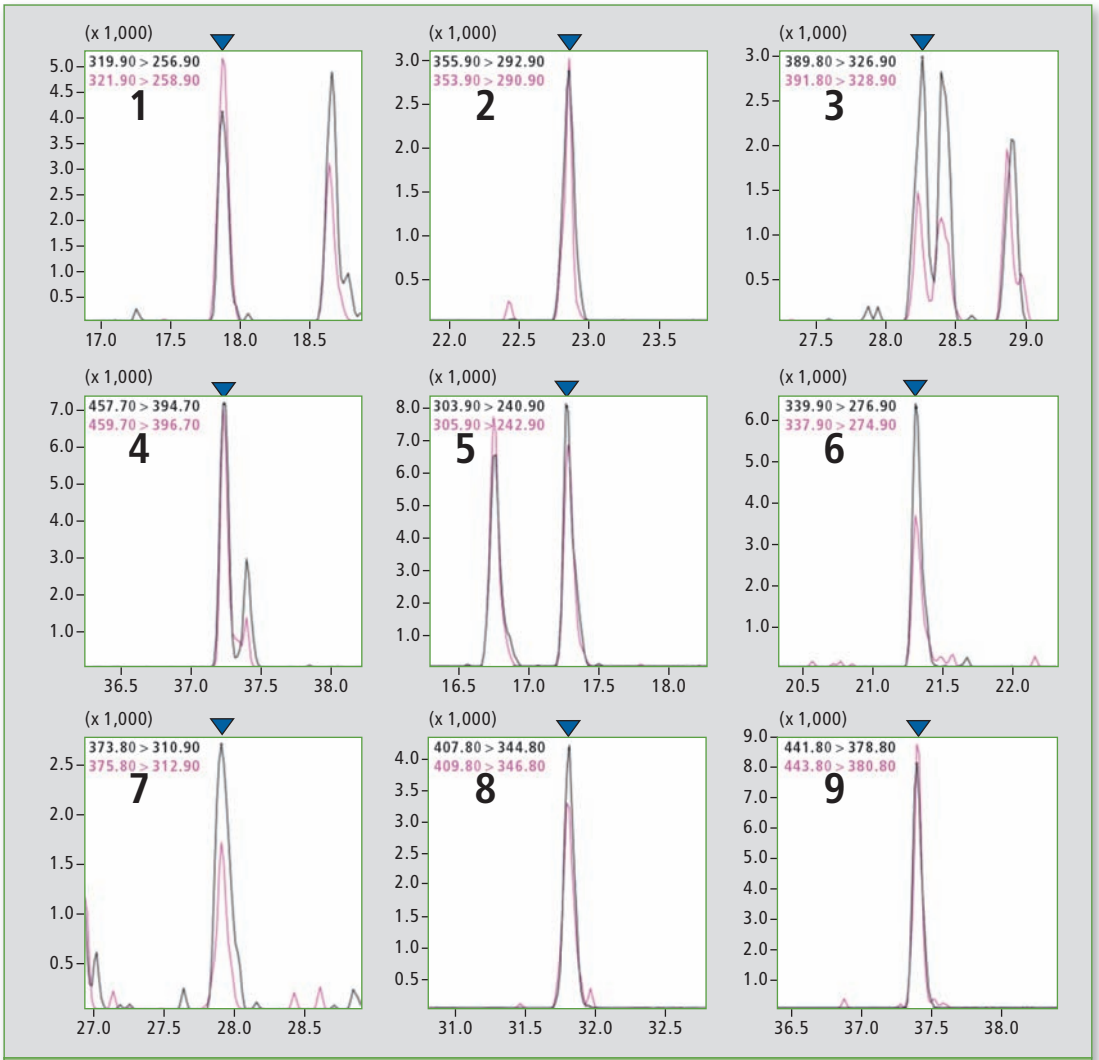

Figure 1: GCMS chromatograms for a concentration of 0.050 pg/uL

trometer uses a high-sensitivity detector, capable of detection at femtogram order concentrations, enabling the analysis of dioxins in foods and feeds. Additionally, the "GC-MS/MS Method Package for Dioxins in Foods" consists of method files registered with optimal conditions for the analysis of dioxins, as well as a report creation tool which documents the items required by EU regulations.

In this article, dioxins (polychlorinated dibenzo-p-dioxin (PCDD) and polychlorinated dibenzofuran (PCDF) only) were analyzed in 44 types and 200 samples of foods and feeds using the GCMS-TQ8050 NX in combination with the method package. Additionally, GC-MS/MS analysis results were compared with those from GC-HRMS in order to evaluate the quantitative capabilities of both techniques.

Method files for the analysis of dioxins

The features of the "EU Regulation Compliant GC-MS/MS Method Package for Dioxins in Foods" are shown below.

- Method files registered with optimal conditions for the analysis of dioxins.
- Retention times and time programs can be adjusted automatically, even when the retention times for the measured compounds change, such as when conducting maintenance of the column tip.
- A report creation tool is included in this product. It can automatically create reports showing items required by EU regulations.

Experiment

For the various food samples, pretreatment was performed using an automatic pretreatment unit (extraction: SpeedExtractor [BUCHI]; purification: GO-xHT [Miura Co., Ltd.]). 10 uL of Nonane was used as final solvent for the samples. For the standard, a mixture of DF-ST and DF-LCS from Wellington Laboratories was used. In terms of the analytical conditions for GC-MS/MS, the conditions registered in the method package were used. Analytical conditions in detail are shown in table 1 (page 19).

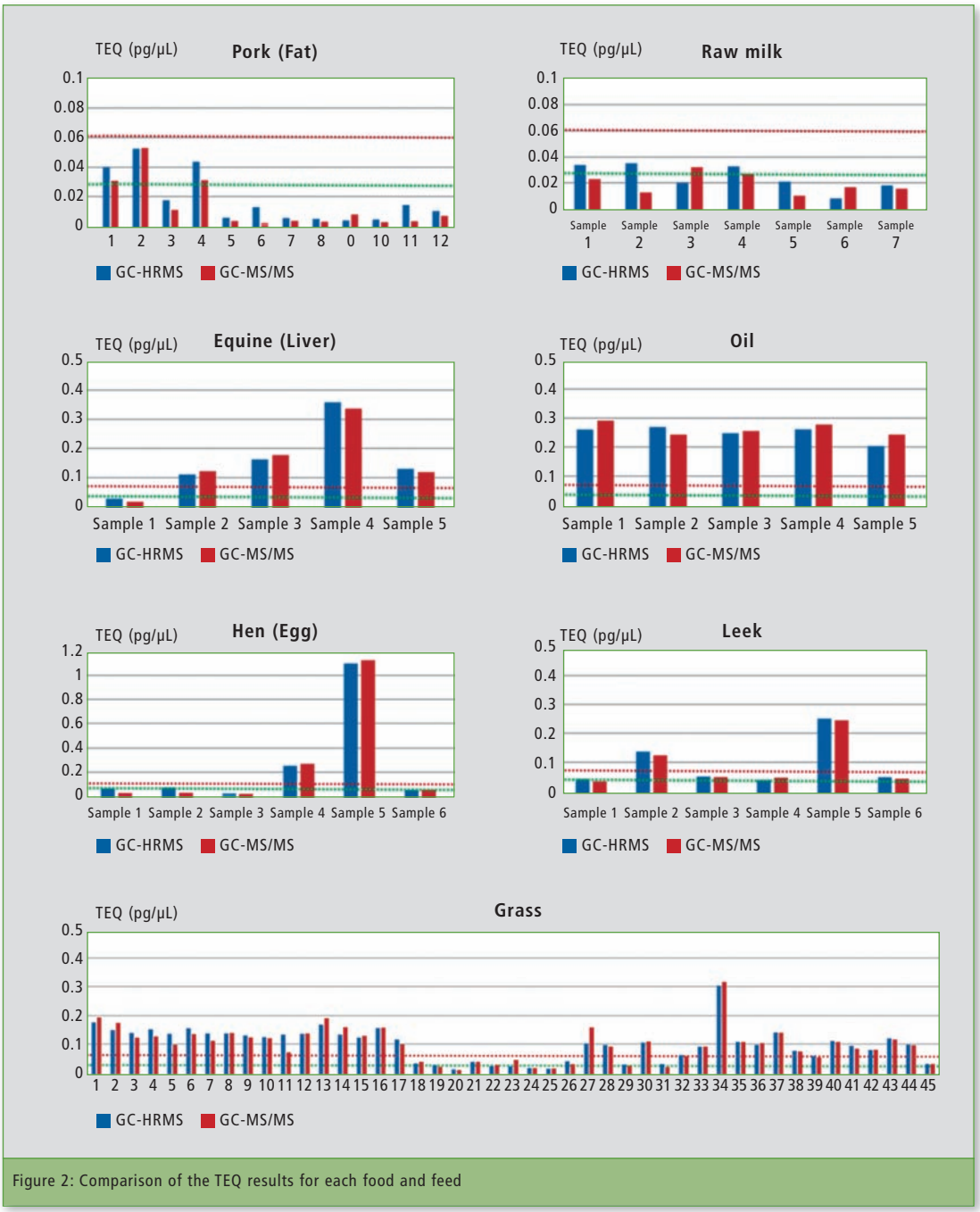

Figure 2: Comparison of the TEQ results for each food and feed

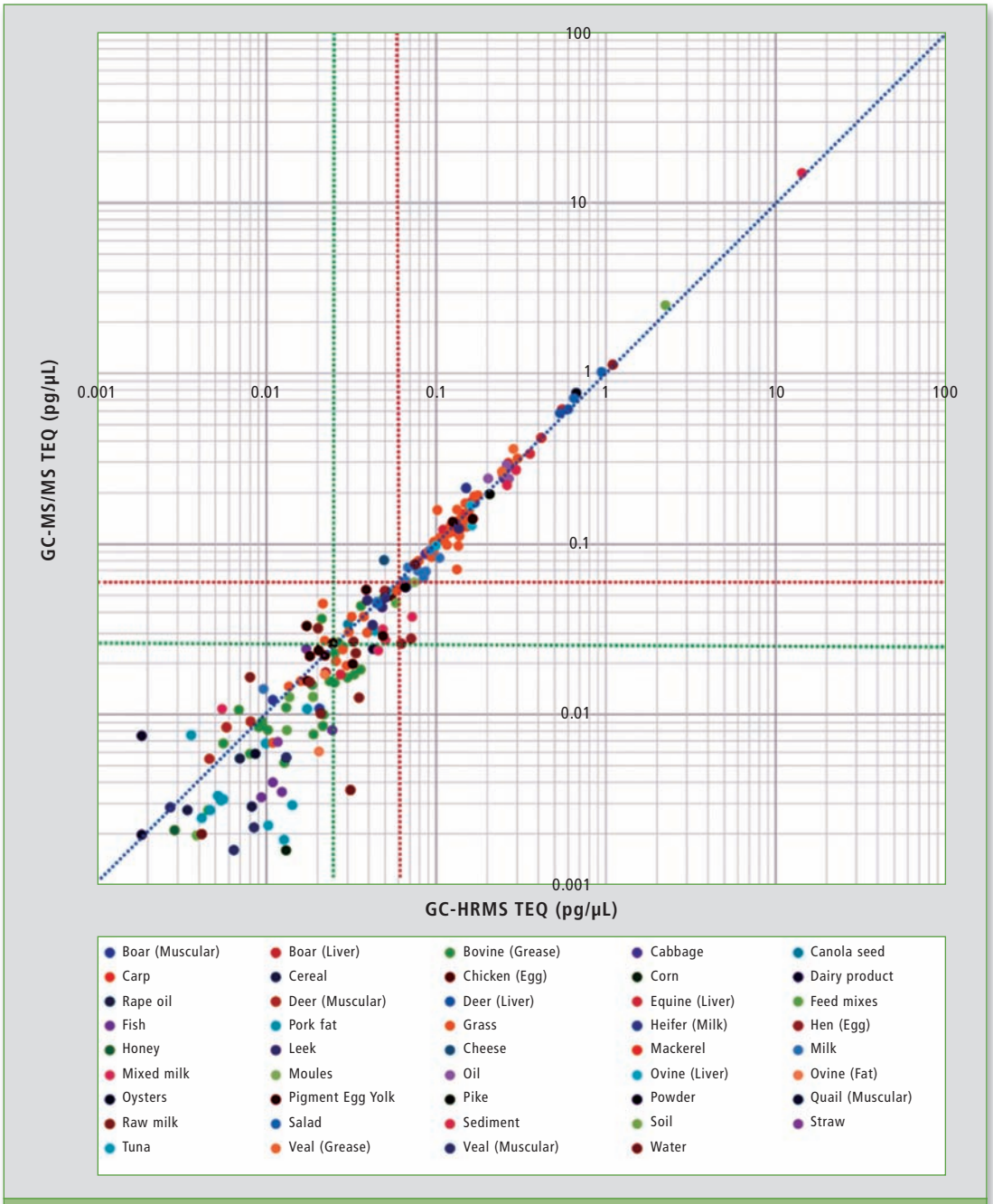

Figure 3: Summarized comparison of the TEQ results for TQ and HR MS

Analysis results for the standards

In the analysis of dioxins in foods, Maximum Levels (ML) are prescribed for each sample. With the food and feed samples in this investigation, ML for pig fat and pig meat were the lowest at 1 pg/g of fat. Additionally, the limit of quantitation (LOQ) required for each compound in the analysis depends on the sample's ML, the pretreatment method and the TEF (toxic equivalence factor) of each compound.

The compounds 2,3,7,8-Tetrachlorodibenzo-p-dioxin and 1,2,3,7,8-Pentachlorodibenzo-p-dioxin have the highest TEF (TEF = 1), requiring lower LOQs than other compounds. In this investigation, the LOQ for both dioxins in pig fat and pig meat was 0.060 pg/uL at the concentration in the final vial.

S/N Ratio (hereinafter »Method 1«)

The concentration of an analyte in the extract of a sample which produces an instrumental response at two different ions to be monitored with an S/N (signal/noise) ratio of 3:1 for the less intensive raw data signal.

Lowest concentration point on the calibration curve (hereinafter »Method 2«)

The lowest concentration point on a calibration curve that gives an acceptable (≤ 30 %) and consistent (measured at least at the start and at the end of an analytical series of samples) deviation from the average relative response factor calculated for all points on the calibration curve in each series of samples. In this technical report, for the purposes of confirmation, an evaluation was performed using both criteria.

As noted above, for 2,3,7,8-Tetrachlorodibenzo-p-dioxin it is necessary to set the LOQ to 0.060 pg/uL or less. Accordingly, the STD was prepared so that the concentration of each compound was 0.050 pg/uL (for Octachlorodibenzo-p-dioxin and Octachlorodibenzofuran 0.100 pg/uL). From the results of the analysis, it was evident that the criteria for method 1 were satisfied for all compounds. S/N ratios for each compound are shown in figure 1 and table 2.

Additionally, with method 2, a calibration curve was created with all six levels used, including 0.025 pg/uL, 0.050 pg/uL, 0.100 pg/uL, 0.250 pg/uL, 0.500 pg/uL and 1 pg/uL. The concentrations for each compound at each calibration curve point (level) are shown in table 3. For each compound, when the level 1 RRF and average RRF were compared, it was found that all compounds satisfied the criteria for method 2. From the above-mentioned results, it was evident that at the LOQ, the criteria were satisfied for all compounds.

Analysis results for the test samples

As previously noted, the level of toxicity differs for each dioxin compound. The TEF, calculated for each compound by taking the toxicity of 2,3,7,8-Tetrachlorodibenzo-p-dioxin as 1, is used as an index of strength. The TEF values for each compound are shown in table 3. The ML for the dioxins in foods and feeds are prescribed by their toxic equivalents (TEQ). The TEQ is calculated by multiplying the concentration of each compound by the TEF and then calculating the total TEQ for all compounds.

Figure 2 (page 17) shows a comparison of the TEQ values for GC-MS/MS and GC-HRMS for food samples. A TEQ of 0.060 pg/uL (red line) and a TEQ of 0.025 pg/uL (green line) are marked as indicators for the samples.

Conclusion

In this technical report, dioxins were analyzed in 44 types and at least 200 samples of foods and feeds using the GCMS-TQ8050 and the "EU Regulation Compliant GC-MS/MS Method Package for Dioxins in Foods". Additionally, the GC-MS/MS analysis results were compared with the analysis results from GC-HRMS in order to assess the quantitative capabilities of both methods. Before analyzing, a STD was measured using GC-MS/MS, and it was confirmed that the criteria were satisfied at the LOQ.

From the above-mentioned results, it is evident that analysis with GCMS-TQ8050 NX and method package provides a quantitative capability equivalent to that of GC-HRMS for samples at the concentration levels required for analysis. However, at concentrations below the required level, differences in quantitative capability could arise. For this reason, it is necessary to be aware of the system status by confirming quantitative capability at the LOQ, and evaluating whether there has been a decrease in sensitivity.

System configuration		Analytical conditions (GC)	
Pretreatment Unit (Extraction)	Speed Extractor (BUCHI)	Insert Liner	Topaz® single gooseneck liner, with wool
Pretreatment Unit (Purification)	GO-xHT (Miura Co., Ltd.)	Column	SH-Rxi™-5Sil MS (60 m, 0.25 mm I.D., 0.25 µm), SHIMADZU
Autosampler	AOC-20i/S	Injection Mode	Splittless
GC-MS/MS	GCMS-TQ-8050 NX	Sampling Time	1.00 min.
Software	GCMSsolution™ Ver. 4.45 SP1	Injection Temp.	280 °C
	LabSolutions Insight™ Ver. 3.2 SP1	Column Oven Temp.	150 °C (1 min) →(20 °C/min) → 220 °C →(2 °C/min) →260 °C (3 min) →(5 °C/min) →320 °C (3.5 min)
	GC-MS/MS method package for dioxins in foods		
Analytical conditions (AOC-20i/s)		HP Injection	450 kPa (1.5 min.)
# of Rinses with Solvent (Pre-run)	3	Flow Control Mode	Linear Velocity (45.6 cm/sec.)
# of Rinses with Solvent (Post-run)	3	Purge Flow	20 mL/min.
# of Rinses with Sample	0	Carrier Gas	Helium
		Analytical conditions (MS)	
Washing Volume	6 µL	Ion Source Temp.	230 °C
Injection Volume	2 µL	Interface Temp.	300 °C
Viscosity Comp. Time	0.2 sec.	Detector Voltage	1.8 kV (Absolute)

Table 1: GC-MS/MS analytical conditions

Nr. of compound in figure 1	Compound name	Calculated S/N
1	2,3,7,8-Tetrachlorodibenzo-p-dioxin	285
2	1,2,3,7,8-Pentachlorodibenzo-p-dioxin	1,658
3	1,2,3,4,7,8-Hexachlorodibenzo-p-dioxin	396
4	Octachlorodibenzo-p-dioxin	2,518
5	2,3,7,8-Tetrachlorodibenzofuran	2,117
6	1,2,3,7,8-Pentachlorodibenzofuran	1,882
7	1,2,3,7,8,9-Hexachlorodibenzofuran	546
8	1,2,3,4,6,7,8-Heptachlorodibenzofuran	1,784
9	Octachlorodibenzofuran	4,282

Table 2: S/N results for standards according to method 1

Compound name	TEF	Avg RRF	RRF (lvl 1)	RRF Dev (%) lvl 1
2,3,7,8-Tetrachlorodibenzo-p-dioxin	1	1.07	1.15	8.1
1,2,3,7,8-Pentachlorodibenzo-p-dioxin	1	1.09	0.97	10.56
1,2,3,4,7,8-Hexachlorodibenzo-p-dioxin	0.1	1.14	1.39	22.26
1,2,3,6,7,8-Hexachlorodibenzo-p-dioxin	0.1	0.95	0.92	2.72
1,2,3,7,8,9-Hexachlorodibenzo-p-dioxin	0.1	1.03	1.25	21.44
1,2,3,4,6,7,8-Heptachlorodibenzo-p-dioxin	0.01	0.92	0.82	11.46
Octachlorodibenzo-p-dioxin	0.0003	1.19	1.04	12.21
2,3,7,8-Tetrachlorodibenzofuran	0.1	1.10	1.05	4.66
1,2,3,7,8-Pentachlorodibenzofuran	0.03	1.04	1.00	3.23
2,3,4,7,8-Pentachlorodibenzofuran	0.3	0.97	0.89	7.59
1,2,3,4,7,8-Hexachlorodibenzofuran	0.1	1.03	0.82	20.72
1,2,3,6,7,8-Hexachlorodibenzofuran	0.1	1.09	1.36	24.62
2,3,4,6,7,8-Hexachlorodibenzofuran	0.1	1.09	1.39	27.83
1,2,3,7,8,9-Hexachlorodibenzofuran	0.1	1.06	1.23	16.10
1,2,3,4,6,7,8-Heptachlorodibenzofuran	0.01	1.17	1.05	10.37
1,2,3,4,7,8,9-Heptachlorodibenzofuran	0.01	1.02	0.97	4.97
Octachlorodibenzofuran	0.0003	1.00	0.84	15.80

Table 3: Each calibration point concentration and RRF for the measured compounds

Speeding up with Velox Core Shell

The new "Velox Core Shell" LC columns offer more application possibilities

So far, the Shim-pack column portfolio has exclusively covered fully porous columns. The new "Shim-pack Velox Core Shell" series closes the gap in the range of columns and thus serves a larger number of application requirements than before. The word velox derives from Latin, meaning "fast" or "quick". It stands for columns with a fast separation performance leading to shorter analysis time when compared to conventional, fully porous columns.

Core Shell technology

Core shell means that the single filling material particles of the column are not fully porous as usual but have a solid core covered with the fully porous material, just like a shell (figure 1). Core shell literally means wrapped core.

Figure 1: Schematic structure of a core shell particle with a solid core (dark blue) and the porous layer (light blue)

The solid core is impermeable to solvents and analytes. This results in a considerably shorter contact time between sample and stationary phase, thus leading to shorter analysis time and higher efficiency of the analysis. One of the characteristics is that the efficiency of a smaller, fully porous particle size (e.g. 1.9 µm) is comparable to a larger particle size of a core shell particle (2.7 µm).

Since system back pressure increases strongly with smaller particles, another benefit of core shell particles is a lower increase of overall pressure, especially when the HPLC system is not very pressure stable and a faster separation is desired. The flow rate can therefore be higher than for columns with fully porous materials. In the following text, these effects are tested in an application.

Measurement parameters and methods

Instrument: LC-2040C 3D (Shimadzu)
Column: Shim-pack Velox C_{18}; (150 mm x 3.0 mm I.D., 2.7 µm); Shim-pack GIST C_{18}; (150 mm x 3.0 mm I.D., 3.0 µm)
Mobile phase: 35 % H_2O; 65 % ACN
Oven temperature: 40 °C
Flow rate: 0.4 mL/min
Injection volume: 0.5 µL

Results

The two chromatograms in figures 2 and 3 demonstrate a comparison of a fully porous column and a Core Shell column. The methods were identical for both columns. The retention times are compared in table 1.

When comparing the figures and the table, it becomes apparent that the Velox-C_{18} column has much shorter retention times than the fully porous GIST-C_{18}. The peak width is also smaller, meaning that

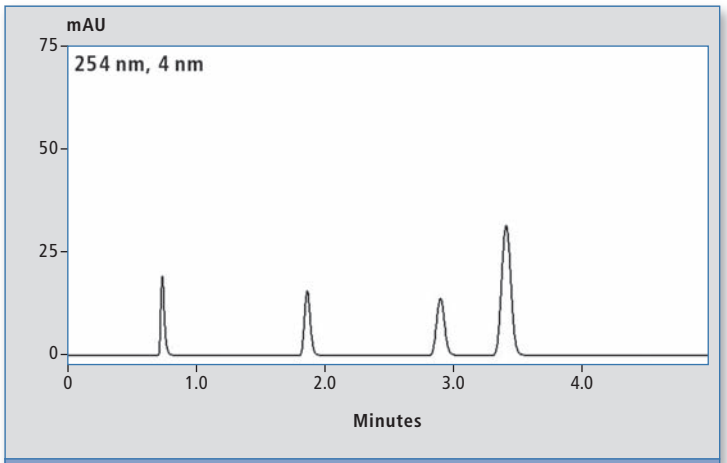

Figure 2: Chromatogram of the GIST-C_{18} column; 3 µm, 150 x 3.0 mm

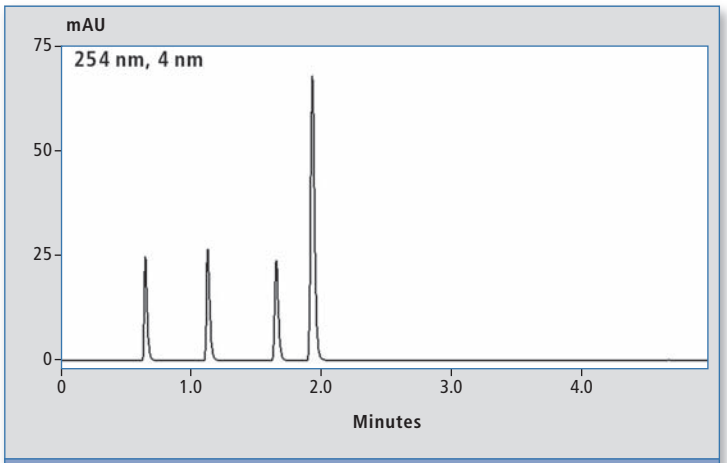

Figure 3: Chromatogram of the Velox C_{18} column; 2.7 µm, 150 x 3.0 mm

the Velox-C_{18} column has a considerably higher efficiency.

In the last peak (naphthalene), retention time and peak width differed significantly. Besides the effect of Core Shell Particles or fully porous particles, this is due to the role of carbon content and the surface of the columns in addition to the column type, which contribute strongly to the retention. The larger the surface area and carbon content on the column, the higher are the interactions between the analytes and the stationary phase, and the higher is the retention. Carbon content is 7 % for the Velox C_{18} column and 14 % for the GIST C_{18} column; surface area is 130 m^2/g (Velox) and 350 m^2/g (GIST). It is clearly visible that the peaks in the Velox column method are much narrower and higher than with the fully porous column.

	t_R (min) Uracil	t_R (min) Methyl benzoate	t_R (min) Toluene	t_R (min) Naphthalene
GIST C_{18}	0.74	1.87	2.90	3.41
Peak width 50 %	0.03	0.05	0.07	0.08
Velox C_{18}	0.65	1.13	1.66	1.94
Peak width 50 %	0.02	0.03	0.03	0.03

Table 1: Retention times and peak widths of GIST C_{18} and Velox C_{18}

Shim-pack Velox portfolio

The Core Shell Velox portfolio covers a wide range of stationary phases and dimensions. A suitable precolumn is also available for each stationary phase. Figure 4 shows all phases with their specifications.

In the following, the different types are shown individually:

Shim-pack Velox SP-C_{18}

SP stands for "sterically protected". Due to the steric protection, the column can be used very effectively for mobile phases in the strongly acidic pH range (pH 1-3). The retention profile is balanced, and the column is also suitable for LC-MS/MS (mass spectrometry) analysis.

Shim-pack Velox C_{18}

This phase is the standard choice for reversed phase chromatography. The Velox C_{18} has the highest hydrophobic retention in the Velox portfolio. It is compatible with slightly acidic to neutral pH values of the mobile phase.

Shim-pack Velox Biphenyl

The biphenyl phase offers complementary selectivity to the alkyl phases. It is suitable for enhanced separation of aromatic compounds. The biphenyl phase is ideal for increasing the sensitivity and selectivity of LC-MS/MS analyses.

Shim-pack Velox PFPP

PFPP stands for pentafluorophenylpropyl. This group provides alternative selectivity for conformational isomers and halogenated compounds. In addition, charged bases are retained more strongly.

Shim-pack Velox HILIC

With Velox-HILIC (Hydrophilic Interaction Chromatography), polar analytes can be retained. The chemical composition of the stationary phase is pure silica. MS sensitivity is increased, partly due to the high organic content that can be used in HILIC mode.

Application

When does it make sense to invest in a Core Shell column? As is often the case, this depends on the application, but also on the existing HPLC device to perform the measurement. Many users use Core Shell columns to convert an existing HPLC method into one with UHPLC characteristics. Fully porous columns with larger particles are replaced by Core Shell columns with smaller particles. The user then benefits from faster analysis without too much back pressure exceeding the limits of the HPLC system. Further advantages are large savings in costs and time.

Since the loading capacity of Core Shell columns is not as high as that of fully porous columns due to the solid core, there is less material in the column with which the sample can interact. If the sample is too highly concentrated, this has a negative effect on the peak shape.

In general, a Core Shell column is suitable if:

- the analysis time should be shorter, without much investment,
- a higher throughput is desired,
- the current HPLC system does not have a system volume that is too high (narrow peaks are widened again by higher system volumes),
- UHPLC columns have an excessively high back pressure or a short service life,
- problems with clogging occur with the current method, or
- loadability is not important.

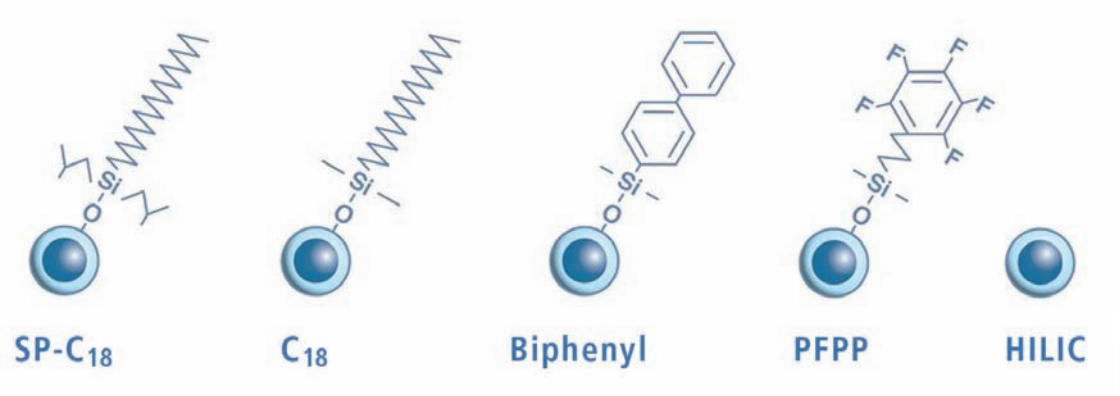

Figure 4: Various stationary phases of the Shim-pack Velox columns

IMPRINT

Shimadzu NEWS, Customer Magazine of Shimadzu Europa GmbH, Duisburg

Publisher
Shimadzu Europa GmbH
Albert-Hahn-Str. 6-10 · D-47269 Duisburg
Phone: +49-203-7687-0
Fax: +49-203-766625
shimadzu@shimadzu.eu
www.shimadzu.eu

Editorial Team
Uta Steeger
Phone: +49 (0)203 76 87-410
Ralf Weber, Maximilian Schulze

Design and Production
m/e brand communication GmbH GWA Duesseldorf

Circulation
German: 5,360 · English: 3,975

Organic plastic in beverage bottles

FTIR analysis of beverage bottles, partly produced from naturally renewable raw materials

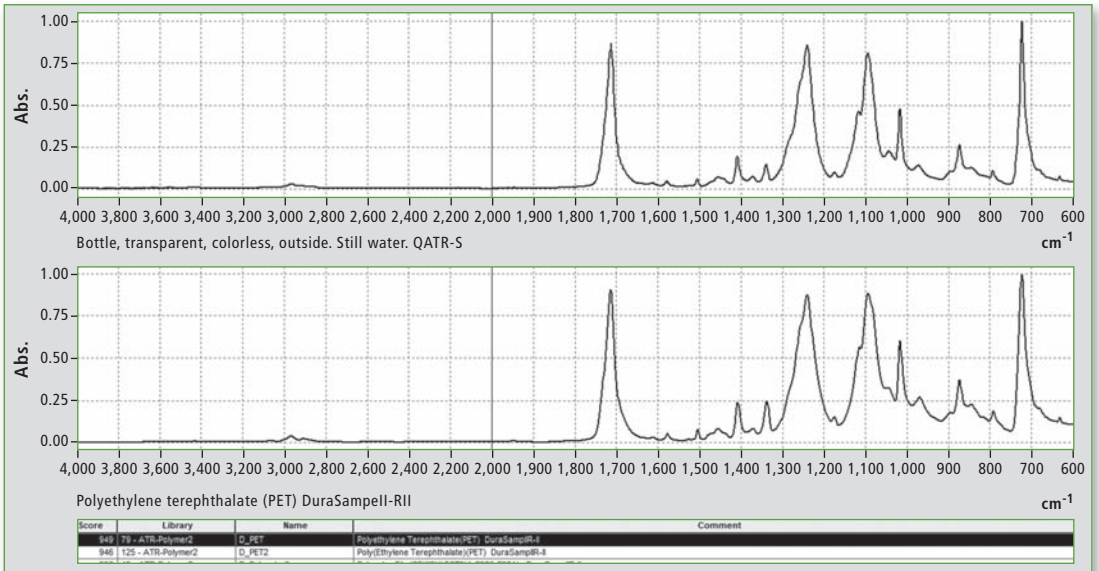

Figure 1: PET spectrum of the plant based raw material bottle identified by the infrared spectrum search in polymer libraries; best hit was found in the ATR polymer library.

Plastic packaging, plastic waste, microplastic and environmental protection – the pollution of nature and the seas by plastic is one of the top issues in the press. Plastic doesn't rot or decay; it takes decades or centuries before it is decomposed by nature.

Among other things, PET, a versatile plastic, is used to make beverage bottles. Despite strong recycling efforts, production has increased from 40 to 56 million tons (2008-16) [1]. That the sturdy polymer-based beverage bottles are made of polyethylene terephthalate (PET) can be read on the bottles. The symbol for PET in recycling is a clearly written 'PET' in the recycling symbol or a '1' in the recycling triangle. This substance can be recycled as waste.

In order to appear more environmentally friendly, alternative plastics from natural basic substances are also used, such as PLA, a plastic based on polylactic acid. However, it does not have the same flexibility as PET in terms of its physical properties (stability, bottles, boxes and foils etc.) PLA used in food applications has up to now been rather stiff and brittle. It can be found in disposable dishes and disposable cups, but it is also used in 3D printers for printing.

Can natural renewable raw materials be 100 % recycled?

It is questionable when about 25 % of a beverage bottle is made from naturally renewable raw materials but is then declared to be 100 % recyclable. To solve this puzzle, FTIR spectroscopy was used because a PET label was found on the beverage bottle.

FTIR spectroscopy allows the substances to be identified. A Shimadzu IRSpirit-T equipped with a diamond-based QATR-S single-reflection unit was used for the analysis. This is possible because the polymers react to heat and the molecular groups of these chemical compounds vibrate.

These vibrations are characteristic for each substance, and they are recorded wave-dependent on the molecular absorption in the range of about 400 to 4,000 cm^{-1} against the molecular absorption to receive a so-called mid infrared spectrum. It can then be identified with the help of libraries.

A/C-PET in the analysis

PET bottles are made of A/C PET. Depending on the wall thickness (soft or hard polymer) and application, PET can contain more amorphous (A-PET) and less crystalline (C-PET) PET or vice versa. The two versions have different FTIR spectra.

Even the PET bottles themselves, which are available on the market, show different ratios of proportions of A- and C-PET. They are also unevenly distributed over the entire bottle body.

The PET variants are usually not the same on the outside, inside or at the bottleneck. The reason is that PET reacts to heat forming with crystallization [2]. The infrared spectrum is further influenced by the arrangement of the molecular structures in the PET and by the manufacturing process of PET as a polymer. This article focuses on PET as A/C PET.

A-PET and C-PET distributed differently

In a separate screening of packaging material, various PET bottles for beverages from Europe and Japan were analyzed. For comparison, 9 samples were used (table 1). In all investigations of PET bottles, a higher proportion of A-PET was found on the outer wall and more of C-PET on the inner wall.

Pure A-PET is rarely found in bottles, which is probably in the nature of PET. Likewise pure C-PET does not exist either (maximum proportion of crystallization is about 75 % [2] [3]). A typical infrared spectrum of these bottles is shown in figure 1. The focus is on the signals at about 1,410 and 1,340 cm^{-1}. Depending on the proportion, the signal at 1,340 cm^{-1} (closer to C-PET) is higher than the signal at 1,410 cm^{-1} (closer to A-PET). Furthermore, shifts of the -CH and CH_2 groups take place, which is evident in the region around 2,900 cm^{-1} (figure 2).

In addition to 'standard bottles', a bottle claiming to be partly made

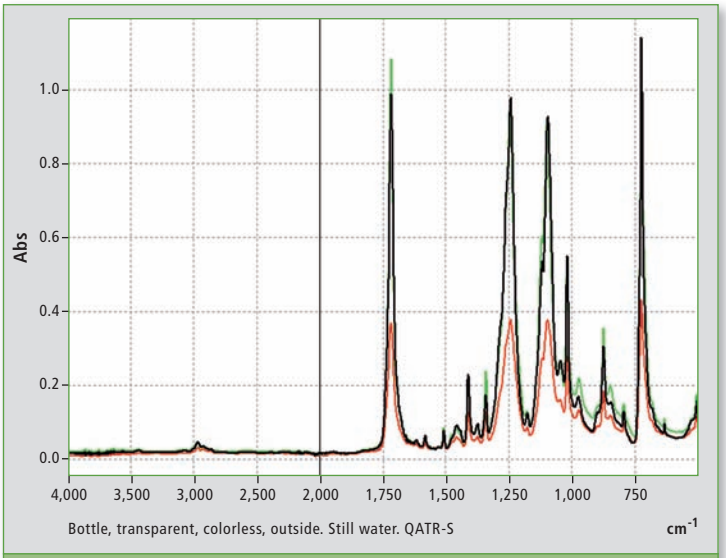

Figure 2: Infrared spectra of a PET-based bottle with the plant based raw materials for still water: Inner wall (green line), outer wall (black line) and a spectrum from the middle (red line) of the bottle wall.

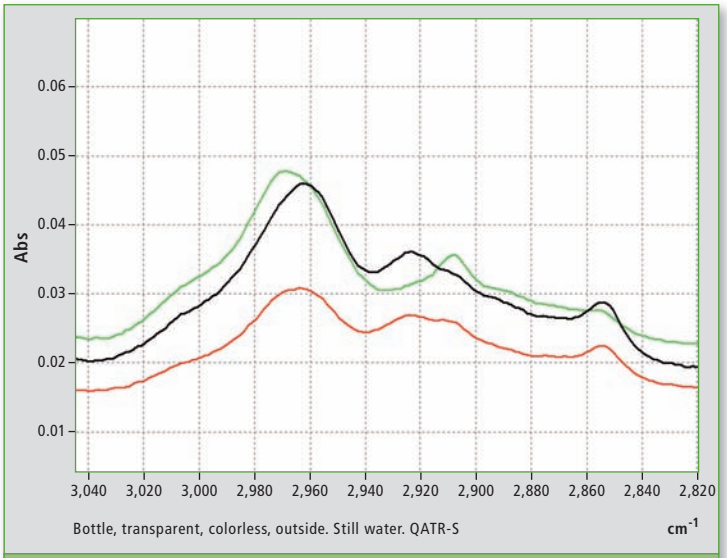

Figure 3: Enlargement from figure 2, range 3,050 to 2,820 cm^{-1}, range of vibration of the aliphatic and aromatic -CH molecular groups [2]

of plant material was also investigated. The bottle wall was cut open and analyzed from both sides using the ATR technique. As the infrared beam enters the surface only to a depth of about 2 µm, the wall was examined in three different ways: inside, in the middle and outside. PET could be found in all three layers. The analysis results of the sample allow better assignment of the signal groups to the PET variants.

The spectra clearly show the different degrees of crystallization of PET. Inner wall and outer wall show differences. The spectrum of the middle layer is the result of the outer and inner wall. After superposition, addition of the two outer surfaces shows approximately the nature of the middle layer (figures 2 to 4).

Conclusion

The actual analysis was meant for the bottle containing plant based raw materials (counter 9 in table 1). Using the library search, it has been identified as PET (figure 1). On the bottle, PET is declared in miniature figure, which was produced up to 22.5 % from renewable raw materials. Is this a paradox on first glance? The solution to the puzzle lies in the development of the starting products for the production of PET, which is produced, for example, from the monomers ethylene glycol and terephthalic acid. According to the manufacturer and readable on the Internet, the PET raw material ethylene glycol is obtained from cane sugar. At this point, plants from nature meet production of a technical material such as PET, which is one of the polymers that can be recycled easily and well after usage.

Bio-plastics are becoming more and more important to the industry, and alternatives to sugar cane are being researched, such as plants that are available worldwide. Nevertheless, the way to 100 percent organic plastic bottles still seems far away. [4]

Product	Origin	Polymer declared
Mineral water with Cola flavor sugar free	GER	PET
Mineral water with lemon flavor	NL	PET
Green tea	JPN	PET
Smoothie	GER	PET
Beer	GER	PET
Tasty Blue water	NL	PET
Mineral water conataining CO_2	NL	PET
Lemonade	JPN	PET
Still mineral water	GER	Bottle with plant based raw materials and miniature symbol for PET (not very apparent)

Table 1: Transparent PET bottles collected after use and examined using ATR infrared spectroscopy. All but one bottle were labeled as polymers of recycling category 01 for PET.

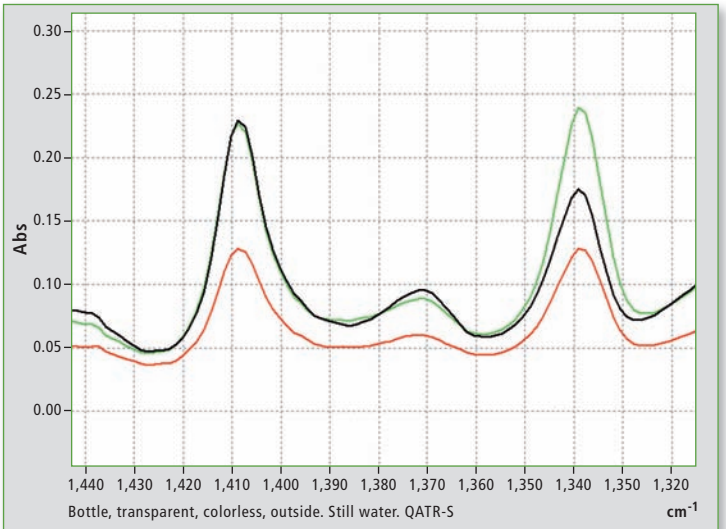

Figure 4: Enlargement from figure 2- range 1,440-1,320 cm^{-1}, range of vibration attributed to ethylene glycol [2]

Literature

[1] https://de.wikipedia.org/wiki/Polyethylenterephthalat
[2] „Plastic Additives Handbook", H. Zweifel et all, 6th edition, Hanser Verlag, 2009.
[3] FTIR spectroscopic analysis of poly(ethylene terephthalate) on crystallization, Ziyu Chen, et all, European Polymer Journal 48(9):1586-1610 September 2012.
[4] https://www.weser-kurier.de/deutschland-welt/deutschland-welt-wirtschaft_artikel,-CocaCola-Bis-2020-alle-Flaschen-aus-Zucker-_arid,1286848.html

New testing methodology for weight reduction

Automotive industry – Case of tensile test with DIC strain analysis of composite material

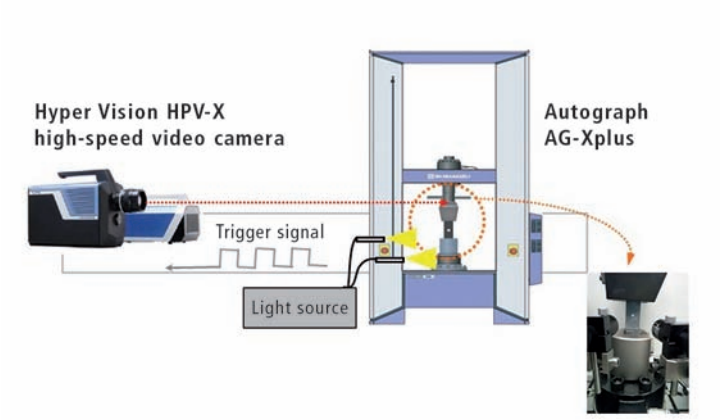

Figure 1: Main unit combined with the HPV-X2 Camera

Improving energy consumption is one of the most important tasks of the automotive market in order to comply with environmental regulations in each country. One of the solutions to solve the problem of energy consumption is weight reduction. It is necessary to achieve it while still securing the safety of the passengers. Various new materials are being developed in order to balance these needs. Looking at metals, these are high-tension steel, aluminium alloys, magnesium alloys and others. With plastics and composite materials such as CFRP (Carbon Fiber Reinforced Plastic) and GFRP (Glass-Fiber Reinforced Plastic), attention is given to combining weight reduction with high-strength properties. Practical usage of several materials has already started in the market, but research is still ongoing.

In the case of composite materials, the internal structure is complicated, so there is a possibility of a failure mode different from conventional materials. If the cause of breakdown can be demonstrated by means of structural analysis simulation, the design of automotive parts using composite materials will greatly advance.
For this reason, it is important to understand the mechanism of occurrence and fracture. A new test method confirming the structure of composite materials is proposed here. In addition, a dedicated example is presented, although several test methodologies exist for composite materials.

Universal testing machine and high-speed video camera

This article explains how to use the precision universal testing machine (Autograph AG-X plus 250 kN) and the high-speed video camera (Hyper Vision HPV-X) (figure 1) to evaluate the static fracture behaviour of a CFRP based on a test force attenuation graph and images of material failure. Information on specimens is shown in table 1. A 6 mm diameter hole is machined in the specimen centre. Fractures are known to propagate easily through composite materials from the initial damage point, and when a crack or hole is present, the material strength is reduced markedly. Therefore, evaluation of the strength of open-hole specimens is extremely important from the perspective of safe application of CFRP materials, e.g. in aircraft and other.

Note:

The CFRP laminate board used in the actual test was created by laying up pre-impregnated material with fibers oriented in a single direction.

The [+45/0/-45/+90]2s shown as the laminate structure in table 1 refers to the laying up of 16 layers of material with fibers oriented at +45°, 0°, -45°, and +90° in two-layer sets.

Testing machine creates signal for camera

In this test, the change in load occuring during specimen fracture was used to trigger the HPV-X high-speed video camera. Specifically, the AG-X plus precision universal testing machine was configured to generate a signal when the test force on the specimen reaches half the maximum test force (referred to as Maximum test force in figure 2), with this signal being sent to the high-speed video camera. Static tensile testing and fracture observation were performed according to the

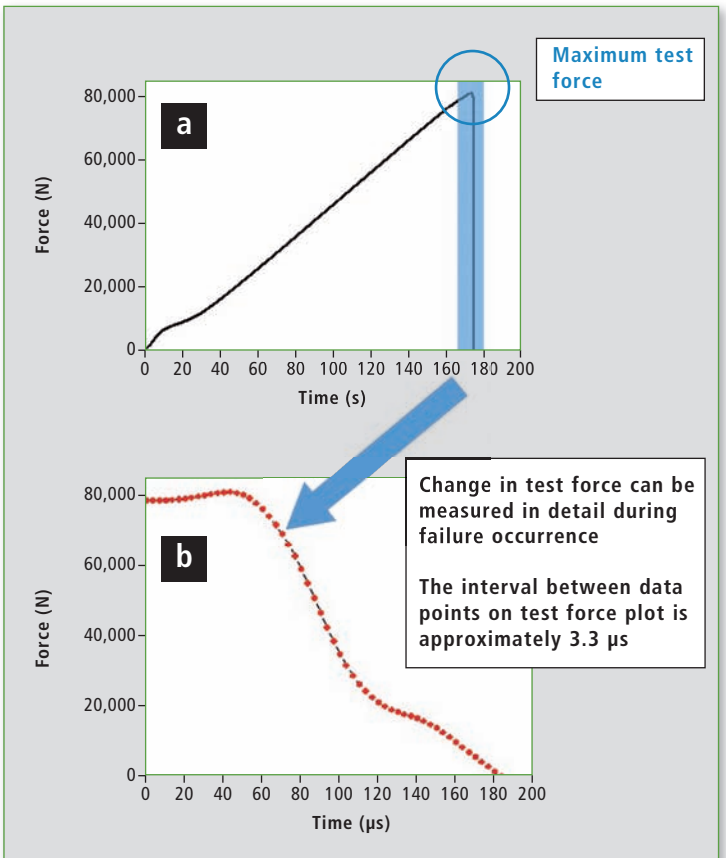

Figure 2: Test graphs

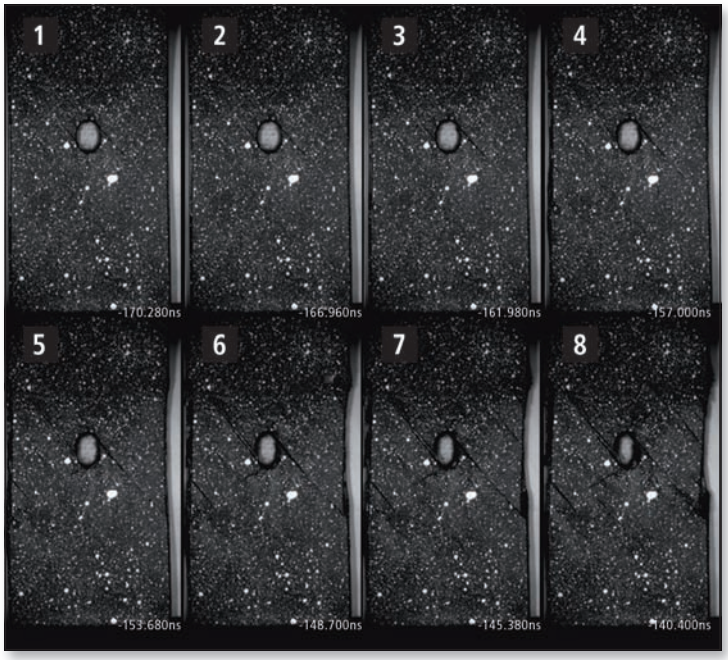

Figure 3: Observation of fracture

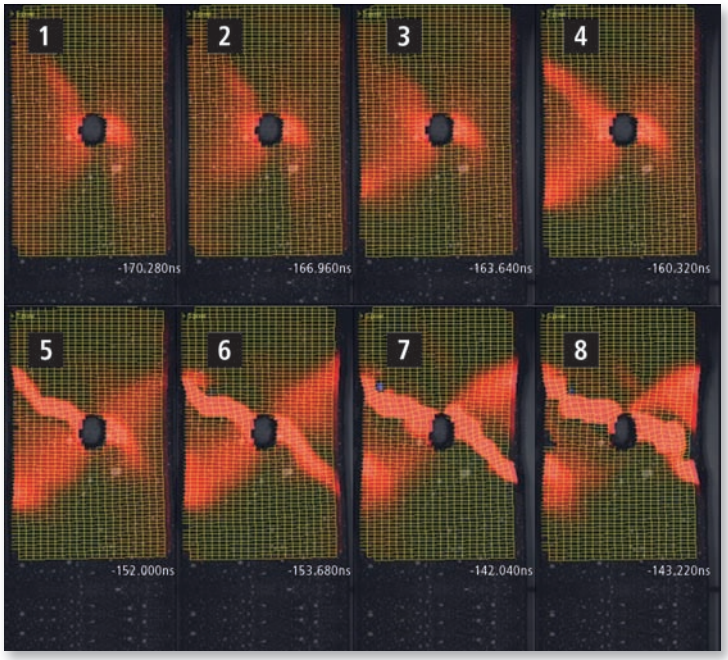

Figure 4: Observation of fracture (DIC analysis)

Laminate structure	Dimensions L (mm) x W (mm) x T (mm), hole diameter (mm)
$[+45/0/-45+90]_{2s}$	150 x 36 x 2.9, Ø6

Table 1: Test specimen information

Testing machine	AG-Xplus
Load cell capacity	250 kN
Jig	Upper: 250 kN non-shift wedge type grips (with trapezoidal file teeth on grip faces for composite materials) Lower: 250 kN high-speed trigger-capable grips
Grip space	100 nm
Loading speed	1 mm/min
Test temperature	Room temperature
Software	TRAPEZIUM X (single)
Fracture observation	HPV-X high-speed video camera (recording speed 600 kfps)
DIC analysis	StrainMaster (LaVision GmbH)

Table 2: Test conditions (*fps stands for frames per second. This refers to the number of frames that can be captured in one second).

conditions shown in table 2. A test force-displacement plot for the open-hole quasi-isotropic CFRP (OH-CFRP) is shown in figure 2a. A test force-time plot during the occurrence of material fracture is also shown in figure 2b.

Figure 2a can be interpreted to show that the specimen fractured at the moment it reached maximum test force, at which point the load on the specimen was suddenly released. This testing system can be used to perform high-speed sampling to measure in detail the change in test force in the region of maximum test force. The time interval between data points on the test force plot in figure 2b is 3.3 µs.

Images 1 through 8 in figure 3 capture the behavior of the specimen during fracture around the circular hole. Image 1 shows the moment cracks occur in a surface +45° layer. In this image, the tensile load being applied is deforming the circular hole, with hole diameter in the direction of the load of approximately 1.4 times that perpendicular to the load. In image 2, cracks occurring around the circular hole are propagating along the surface +45° layer. In images 3 through 6, a substantial change can be observed in the external appearance of the specimen near the end of the crack propagating to the bottom right from the circular hole. This suggests that not only the surface layer, but internal layers are also fracturing. Based on the images of the same area and the state of the internal layers that can be slightly observed from the edges of the circular hole in images 7 and 8, the internal fracture has propagated quickly in the 18 µs period between images 3 and 8.

Digital Image Correlation (DIC) analysis

DIC analysis performed on the fracture observation images of figure 3. Black signifies areas of the surface layer of the specimen under little strain, and red signifies areas under substantial strain. Looking at images 1 through 4 (in figure 4), it can be seen that strain around the circular hole is focused diagonally toward the top-left (-45 °) and toward the bottom-left (+45 °) from the circular hole. Images 5 through 8 show the focusing of strain diagonally toward the bottom-right (-45 °) and toward the top-right (+45 °) from the circular hole in areas where it was not obvious in images 1 through 4. This shows that an event is occurring in the surface layer of the specimen that is similar to the process of fracture often seen during tensile testing of ductile metal materials, i.e. crack propagation in the direction of maximum shear stress.

Ethanol as a blending component for petrol

Determination of higher alcohols and volatile impurities by gas chromatographic method

Researchers have been experimenting with alternative fuels due to steadily increasing demand and decreasing supply of petroleum crude oil. Ethanol has been recognized as a possible liquid fuel alternative which can be available in significant quantities throughout the remainder of this century [1].

GC-2010 Plus

Ethanol blending is a process of mixing ethanol with petrol to enhance the octane content in fuel. This procedure reduces engine carbon monoxide (CO) and carbon dioxide emissions by up to 30 %. Moreover, it improves engine operation since it acts as an anti-knock agent [2].

Researchers have used ethanol as a component in conventional petroleum fuels because it has a higher thermal efficiency than ordinary petroleum motor fuels. Another benefit is its lower risk of fire during storage and transportation compared to petroleum, which has greater volatility and lower flash point than ethanol.

The EN 15721 European Standard relates to the determination of several compounds that may be present in ethanol at different concentration levels. The target compounds are separated into the following groups:

a) Higher alcohols:
propan-1-ol, butan-1-ol, butan-2-ol, 2-methylpropan-1-ol (isobutanol), 2-methylbutan-1-ol, 3-methylbutan-1-ol. The compounds of the first group can be determined up to 3 % (m/m).

b) Impurities:
ethanol (acetic aldehyde), ethylethanoate (ethyl acetate), 1,1-diethoxy ethane (acetal) are specified up to 2 % (m/m).

This gas chromatographic method includes the determination of a test portion with split injection mode into a gas chromatograph (GC) system. Addition of pentan-3-ol to the sample is the only sample pretreatment step. The sample is then introduced to the gas chromatograph (GC) system using split injection mode. A Flame Ionization Detector (FID) is used for the detection of the analytes.

Apparatus

Gas chromatograph: Shimadzu GC 2010 Plus, Split/Splitless injector, FID detector
Capillary column: DB-1701 (60 m × 0.25 mm ID, 1.00 µm film thickness)

Two calibration stock solutions are used for the preparation of calibration standards and control samples. The first solution (catalogue number EN 15721-A) contains the ten target-compounds at 1 % (m/m) and the second (catalogue number EN 15721-A-IS) contains the internal standard (1 % m/m pentan-3-ol).

Calibration solution and sample preparation

Preparation of Calibration solution: 1 mL of ethanol is transferred into a 2 mL vial and is weighed to the nearest 0.1 mg. 100 uL of calibration stock solution (catalogue number EN 15721-A) is added and mass is recorded to the nearest 0.1 mg. 80 uL of internal standard stock solution (catalogue number EN 15721-A-IS) is added and mass is recorded to the nearest 0.1 mg [3].

Sample Preparation: 1 mL of sample is transferred into a 2 mL vial and is weighed to the nearest 0.1 mg. 80 uL of internal standard stock solution (catalogue number EN 15721-A-IS) is added and mass is recorded to the nearest 0.1 mg [3].

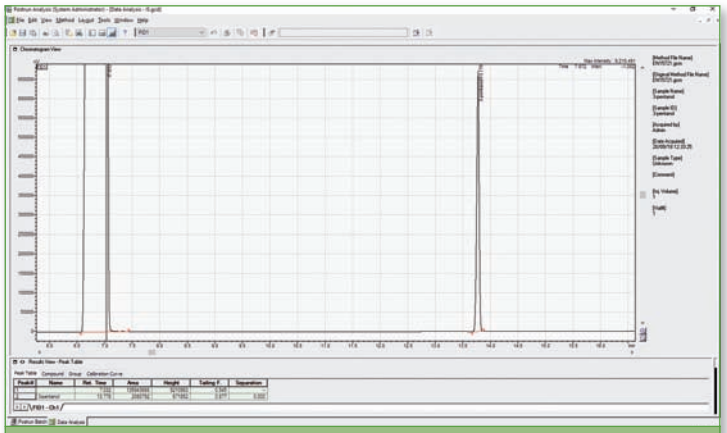
Figure 1: Chromatogram of 3-pentanol (ISTD)

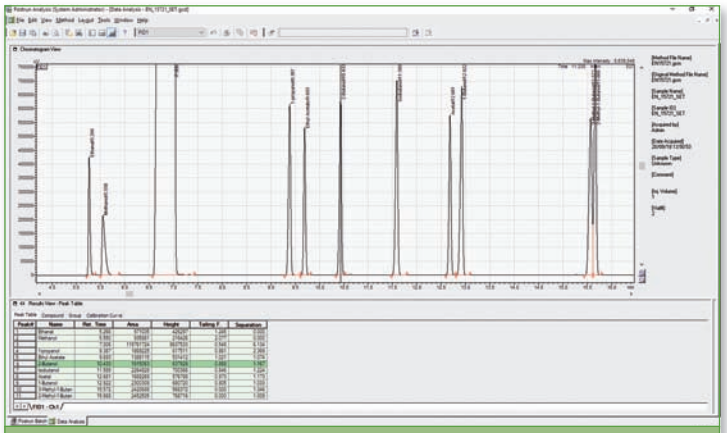
Figure 2: Chromatogram of calibration stock solution

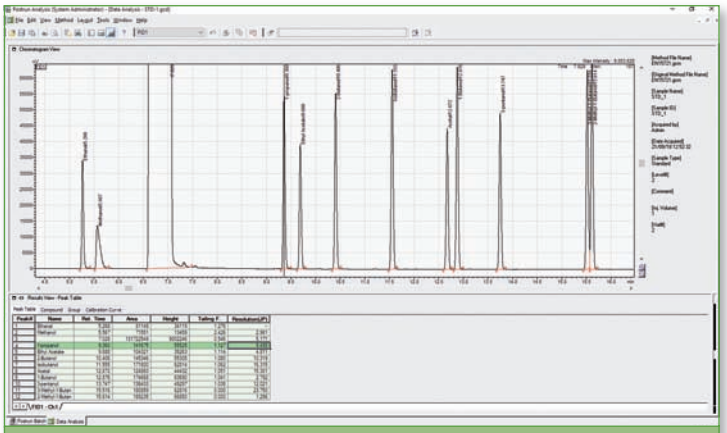

Figure 3: Chromatogram of calibration solution

Results and discussion

Chromatograms

The analysis was started with the injection of internal standard stock solution (catalogue number EN 15721-A-IS) and the injection of calibration stock solution since retention times of all compounds should be determined.

The next step was the analysis of Calibration Standard Solution to confirm compliance with the acceptance criteria, as far as chromatographic resolution is concerned. Baseline separation was obtained for all components except for 2-methylbutan-1-ol and 3-methyl-butan-1-ol (R = 1.3, R ≥ 1.0 is the EN 15721 specification).

Calibration curve

The Calibration Standard Solution was injected three times to obtain a two-point calibration curve (y = a x) for each analyte. The desired repeatability levels were achieved since the % RSD was 0.0 - 0.5 % (% RSD ≤ 5.0 is the EN 15721 specification) for both area ratio and response factor results of three calibration standard injections.

Expression of results

Results were calculated through the GC solution software according to the following equations:

Resolution: $R = 2 (t_2 - t_1) / 1{,}699 (W_1 + W_2)$
Response Factor: RF = Area (ISTD) x C (compound) / Area (compound) x C (ISTD)
Impurities: Q = ethanol + ethyl-ethanoate + 1,1-diethoxyethane + oxygenated compounds
Methanol: Cm = methanol content
Higher alcohols: Ch = propan-1-ol + butan-1-ol + butan-2-ol + 2-methylpropanol + 2-methylbutan-1ol +3-methylbutan-1-ol

Concentration is expressed in g/100 g, % (m/m).

Conclusion

The EN 15721 standard was successfully applied with the GC-2010 Plus. The appropriate use of the instrument and the accurate application of EN 15721 resulted in chromatograms with an acceptable number of theoretical plates while the presence of the AOC-20i auto-sampler contributed to the excellent repeatability.

Selection of an appropriate column was critical to achieve acceptable resolution (R_s > 1.0) between 2-methyl-1-butanol and 3-methyl-1-butanol. Also, the chromatographic method parameters of EN 15721 and the adoption of default values in gas flow rates for the detector (FID) ensured that all acceptance criteria of the Standard were fulfilled.

Finally, proper maintenance of the injection port and column oven before analysis helped to obtain chromatograms with low noise levels and high S/N values for the target-compounds.

Part of GC	Values
Split injector temperature	200 °C
Split ratio	50
FID temperature	260 °C
FID air flow	400 mL/min
FID hydrogen flow	40 mL/min
FID make-up flow	30 mL/min
Carrier gas	He
Linear velocity	22 cm^3/sec
Column flow	1.4 mL/min
Oven temperature program	40 °C → 1 min 5 °C → 250 °C → 2 min

Table 1: Method parameters

Calibration compounds	Description
Methanol	—
Propan-1-ol	Higher alcohols
Butan-1-ol	Higher alcohols
Butan-2-ol	Higher alcohols
2-methylpropanol	Higher alcohols
2-methylbutan-1-ol	Higher alcohols
3-methylbutan-1-ol	Higher alcohols
Ethanal (acetic aldehyde)	Impurity
Ethyl-ethanoate (ethyl acetate)	Impurity
1,1-diethoxy ethane (acetal)	Impurity
Pentan-3-ol	Internal standard
Ethanol	Solvent

Table 2: Reagents and materials

Compound	Retention time (min)	LOD (% m/m)	LOQ (% m/m)
Ethanal	5.268	0.0009	0.0028
Methanol	5.567	0.0002	0.0006
1-propanol	9.360	0.0006	0.0019
Ethyl acetate	9.680	0.0017	0.0050
2-butanol	10.406	0.0002	0.0006
Isobutanol	11.555	0.0003	0.0009
Acetal	12.672	0.0006	0.0017
1-butanol	12.876	0.0001	0.0002
3-methyl-1-butanol	15.516	0.0003	0.0010
2-methyl-1-butanol	15.614	0.0002	0.0006
3-pentanol (ISTD)	13.747	—	—

Table 3: Compound table

Authors

Fotis Fotiadis, Georgia Flessia,
Dr. Gerasimos Liapatas,
Dr. Manos Barbounis
N.Asteriadis S.A.,
Athens, Greece

Literature

[1] G. Najafi, B. Chobadian, T. Tavakoli, D.R. Buttsworth, T.F. Yusaf, M. Faizollhnejad, Appl. Energy 86 (2009) 630-639.

[2] Y. Barakat, Ezis N. Awad, V. Ibrahim, Egyptian Petroleum Research Institute (EPRI), Egypt (2016), "Fuel consumption of gasoline ethanol blends at different engine rotational speeds"

[3] EUROPEAN STANDARD EN 15721 "Ethanol as a blending component for petrol – Determination of higher alcohols, methanol and volatile impurities – Gas chromatographic method"

Pyrolysis GC-MS user meeting

March 28, 2019, at Shimadzu's Laboratory World, Duisburg, Germany

Take this opportunity for detailed discussions with experts from research and industry on the numerous pyrolysis GC-MS applications.

The all-day event offers a varied program with lectures and practical examples as well as cutting-edge information on instrument technology and applications. In addition, the tour around Shimadzu's Laboratory World provides insights into this high-end testing facility for the entire analytical instrumentation product range on over 1,500 m².

However, there will be sufficient time for sharing experiences and for discussions during the breaks.

We look forward to welcoming you to this special event in Duisburg!

For further information, please use the link below:

www.shimadzu.eu/Pyrolysis-User-Meeting

GCMS-QP2020 NX

Shimadzu live

Anakon
Münster, Germany
March 25 - 28, 2019
www.gdch.de/anakon2019

Forum Labo
Paris, France
March 26 - 28, 2019
www.forumlabo.com/

Pyrolysis User Meeting
Duisburg, Germany
March 28, 2019
www.shimadzu.eu/Pyrolysis-User-Meeting

Euromedlab
Barcelona, Spain
May 19 - 23, 2019
www.euromedlab2019barcelona.org

Automotive
Stuttgart, Germany
May 21 - 23, 2019
www.testing-expo.com/europe/en/

PEFTEC
Rotterdam, Netherlands
May 22 - 23, 2019
www.ilmexhibitions.com/peftec/

@ShimadzuEurope

NEWS – print and digital

Print version: If you would like to receive the **Shimadzu News** on a regular basis, please email us your postal address via: **shimadzu-news@shimadzu.eu**

Also as App: the Shimadzu NEWS is also available as WebApp via **www.shimadzu-webapp.eu**

You can also subscribe to our **newsletter** via: **www.shimadzu.eu/newsletter**